ResearchGate

See discussions, stats, and author profiles for this publication at: https://www.researchgate.net/publication/275668948

Multitarget Therapeutic Leads for Alzheimer's Disease: Quinolizidinyl Derivatives of Bi- and Tricyclic Systems as Dual Inhibitors of Cholinesterases and -Amyloid (A) Aggregation

ARTICLE *in* CHEMMEDCHEM · APRIL 2015

Impact Factor: 2.97 · DOI: 10.1002/cmdc.201500104 · Source: PubMed

CITATIONS
2

READS
54

13 AUTHORS, INCLUDING:

Michele Tonelli
Università degli Studi di Genova
22 PUBLICATIONS **237** CITATIONS
SEE PROFILE

ANGELO DE STRADIS
Italian National Research Council
173 PUBLICATIONS **769** CITATIONS
SEE PROFILE

Vito Boido
Università degli Studi di Genova
62 PUBLICATIONS **505** CITATIONS
SEE PROFILE

Angelo Carotti
Università degli Studi di Bari Aldo Moro
225 PUBLICATIONS **4,135** CITATIONS
SEE PROFILE

Available from: ANGELO DE STRADIS
Retrieved on: 13 January 2016

ChemPubSoc Europe

DOI: 10.1002/cmdc.201500104

CHEMMEDCHEM Full Papers

Multitarget Therapeutic Leads for Alzheimer's Disease: Quinolizidinyl Derivatives of Bi- and Tricyclic Systems as Dual Inhibitors of Cholinesterases and β-Amyloid (Aβ) Aggregation

Michele Tonelli,*[a] Marco Catto,*[b] Bruno Tasso,[a] Federica Novelli,[a] Caterina Canu,[a] Giovanna Iusco,[a] Leonardo Pisani,[b] Angelo De Stradis,[c] Nunzio Denora,[b] Anna Sparatore,[d] Vito Boido,[a] Angelo Carotti,[b] and Fabio Sparatore[a]

Multitarget therapeutic leads for Alzheimer's disease were designed on the models of compounds capable of maintaining or restoring cell protein homeostasis and of inhibiting β-amyloid (Aβ) oligomerization. Thirty-seven thioxanthen-9-one, xanthen-9-one, naphto- and anthraquinone derivatives were tested for the direct inhibition of Aβ(1–40) aggregation and for the inhibition of electric eel acetylcholinesterase (eeAChE) and horse serum butyrylcholinesterase (hsBChE). These compounds are characterized by basic side chains, mainly quinolizidinylalkyl moieties, linked to various bi- and tri-cyclic (hetero)aromatic systems. With very few exceptions, these compounds displayed inhibitory activity on both AChE and BChE and on the spontaneous aggregation of β-amyloid. In most cases, IC_{50} values were in the low micromolar and sub-micromolar range, but some compounds even reached nanomolar potency. The time course of amyloid aggregation in the presence of the most active derivative ($IC_{50} = 0.84$ μM) revealed that these compounds might act as destabilizers of mature fibrils rather than mere inhibitors of fibrillization. Many compounds inhibited one or both cholinesterases and Aβ aggregation with similar potency, a fundamental requisite for the possible development of therapeutics exhibiting a multitarget mechanism of action. The described compounds thus represent interesting leads for the development of multitarget AD therapeutics.

Introduction

Alzheimer's disease (AD) is a progressive neurodegenerative disorder characterized by the accumulation of aggregates of β-amyloid (Aβ) and hyperphosphorylated tau proteins leading to the formation of extracellular amyloid plaques and intracellular fibrillary tangles, respectively. Aβ exists as a mixture of two prevalent peptides, Aβ(1–40) and Aβ(1–42), containing 40 and 42 amino acids, respectively, with the latter being the most prompt to aggregate and the most cytotoxic in humans. It is accepted that soluble, low-molecular-weight oligomers formed as intermediate species in the aggregation process of Aβ are responsible for neuronal damage and ultimately cell death. These events have been challenged by the "cholinergic hypothesis" that associates the main cognitive and behavioral symptoms of AD to the loss of cholinergic neurons and the consequent low synaptic levels of the neurotransmitter acetylcholine (ACh).[1] Current symptomatic therapies of AD rely on the restoration of ACh levels through the inhibition of acetylcholinesterase (AChE), the enzyme responsible for the hydrolysis of ACh at its catalytic anionic site (CAS). Indeed, it has been shown that AChE, at its peripheral anionic binding site (PAS), might promote the aggregation of Aβ.[2] Therefore, dual binding site inhibitors of AChE could be beneficial in relieving cognitive and behavioral symptoms of AD by reducing both ACh hydrolysis and Aβ aggregation. In progressive AD, AChE levels in the brain decline while butyrylcholinesterase (BChE) levels progressively increase. BChE is also able to hydrolyze ACh, but at a lower rate. Selective BChE inhibitors have been reported to increase the ACh level in the brain and also decrease the formation of Aβ.[3]

To obtain novel dual cholinesterase (ChE) inhibitors, or rather BChE-selective inhibitors, we previously prepared a number of compounds derived from phenothiazine and other related tricyclic systems linked by different kinds of spacers to the bulky, lipophilic and strongly basic quinolizidine ring.[4] It is worth noting that even simple derivatives of the quinolizidine ring (that differentiates the novel compounds from the classic BChE inhibitors such as ethopropazine and

[a] Dr. M. Tonelli, Dr. B. Tasso, Dr. F. Novelli, Dr. C. Canu, Dr. G. Iusco, Prof. V. Boido, Prof. F. Sparatore
Dipartimento di Farmacia
Università degli Studi di Genova, V. le Benedetto XV, 3, 16132 Genova (Italy)
E-mail: michele.tonelli@unige.it

[b] Dr. M. Catto, Dr. L. Pisani, Dr. N. Denora, Prof. A. Carotti
Dipartimento di Farmacia-Scienze del Farmaco
Università degli Studi di Bari "Aldo Moro", V. Orabona 4, 70125 Bari (Italy)
E-mail: marco.catto@uniba.it

[c] Dr. A. D. Stradis
Istituto di Virologia Vegetale del CNR
Università degli Studi di Bari "Aldo Moro", V. Amendola 165A, 70126 Bari (Italy)

[d] Prof. A. Sparatore
Dipartimento di Scienze Farmaceutiche "P. Pratesi"
Università degli Studi di Milano, V. Mangiagalli 25, 20133 Milano (Italy)

© 0000 Wiley-VCH Verlag GmbH & Co. KGaA, Weinheim

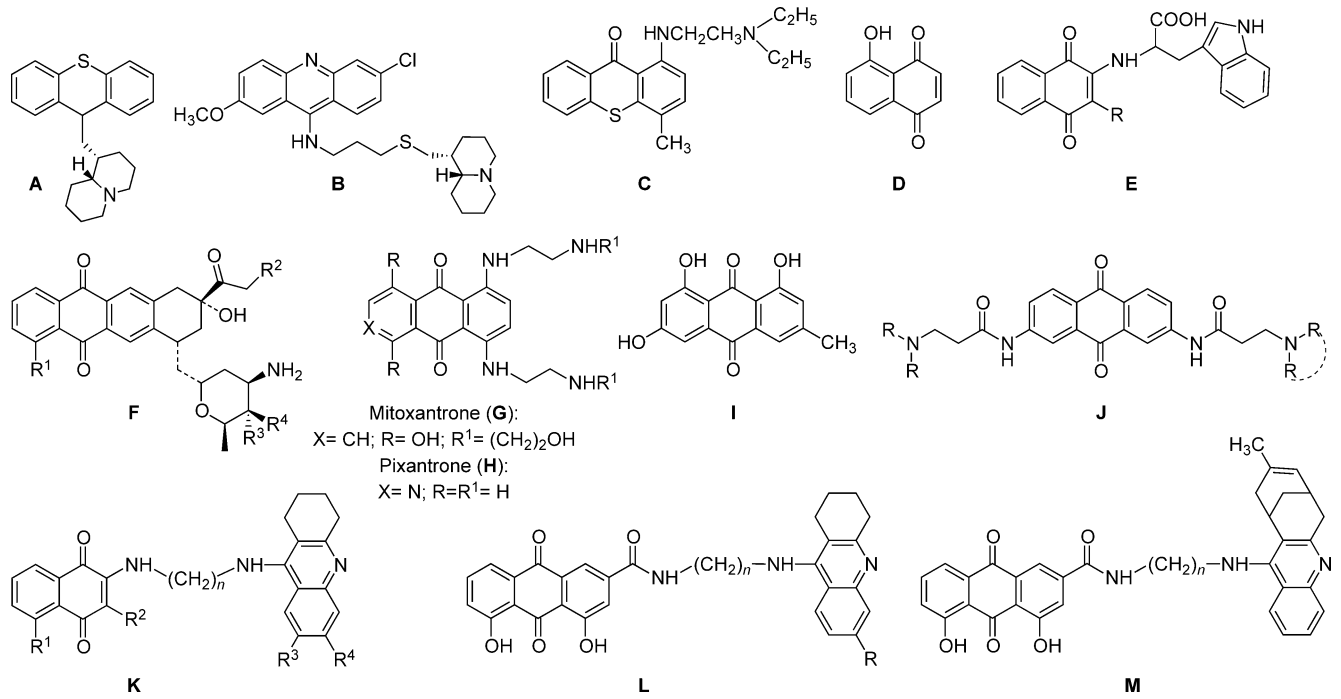

Figure 1. Previously studied compounds.

Astra1397[5]) are endowed with some anti-ChE activity.[6] All the examined compounds[4] exhibited activity against both ChEs, but inhibition of BChE was generally stronger, with sub-micromolar IC_{50} values for most of them. 9-[(Quinolizidin-1-yl)methyl]-thioxanthene (9-lupinylthioxanthene; **A**) was the most potent and selective inhibitor for BChE ($IC_{50}=0.15$ μM; SI = 47; SI is the selectivity index measured as the ratio IC_{50}AChE/IC_{50}BChE). The elongation of the spacer improved the inhibition of AChE; however, this prevailed over BChE inhibition only for 6-chloro-2-methoxy-9-{N-[3-(quinolizidin-1-yl)methylthio]propylamino}-acridine **B** ($IC_{50}=0.22$ μM; SI = 0.32) (**A** and **B** in Figure 1).

Aside from the valuable inhibitory activity of ChEs, several of the studied compounds have shown additional pharmacological properties that could reinforce central cholinergic activity or improve certain cognitive performances in AD. Pursuing the aim to obtain ChE inhibitors with additional pharmacological properties of potential utility in the control of symptoms and/or progression of AD, we turned our attention to quinolizidinyl derivatives of: a) other tricyclic systems as thioxanthen-9-one and xanthenone, and b) bi- and tricyclic quinoid compounds (naphtho- and anthraquinones). Our main goal was the identification of new and potent ChE inhibitors, which also exhibit direct inhibition of Aβ self-aggregation.

The first subgroup of compounds examined is structurally related to lucanthone (**C**), a drug largely used in former times for the treatment of schistosomiasis[7] and that has also been studied as an antitumor agent.[8] Its activity has been related to DNA intercalation, the inhibition of nucleic acid biosynthesis, topoisomerase II and apurinic endonuclease-1 (Ape-1) without affecting its redox activity.[9] More recently, lucanthone has also been shown to disrupt lysosomal function and to inhibit cell autophagy.[10] Autophagy is a degradative process that eliminates anomalous proteins and protein aggregates, thereby maintaining protein homeostasis. Under metabolic and/or hypoxic stress conditions, cells might undergo self-digestion to generate ATP and other essential molecules, thus promoting their own survival. On the other hand, it has been shown that Aβ can be generated in autophagic vacuoles,[11] thus counterbalancing the neuroprotective potential of autophagy. While inhibition of autophagy has been demonstrated to play a role in cancer therapy (by accelerating death of cancer cells typically in a state of nutrient and oxygen deprivation), adequate autophagy modulation might decrease the production of Aβ in AD. Besides this, of particular relevance for the present work is lucanthone's potent inhibition of horse serum BChE (hsBChE; $IC_{50}=0.15$ μM)[12] associated with only a modest inhibition of electric eel AChE (eeAChE; 25–40% at 10 μM) rendering this drug an interesting multitarget lead for AD therapy. The second subgroup of compounds is related to several naphtho- and anthraquinones that have been shown to affect important biological targets. Specifically, compound E3330 and related naphthoquinones[9b,13] inhibit (in contrast to lucanthone) the redox function of Ape-1 while other naphthoquinones, such as juglone (**D**), inhibit Aβ oligomerization[14] without inhibiting fibrillization. Oligomerization and fibrillization might be seen as independent pathways and soluble, low-molecular-weight amyloid oligomers are the primary toxic species in neurodegenerative diseases.[15] The linking of a naphthoquinone moiety to the amino group of tryptophan produced potent inhibitors (**E**) of both oligomerization and fibrillization.[16] Antitumor anthraquinones such as rubicins (**F**)[17] and xanthrones (e.g., mitoxantrone (**G**) and pixantrone (**H**)[18]) proved to be effective Aβ oligomerization inhibitors, with the latter also reducing the cellular toxicity of Aβ peptide.

© 0000 Wiley-VCH Verlag GmbH & Co. KGaA, Weinheim

Interestingly, poly-hydroxyanthraquinones (e.g., emodin (**I**), 1,2,5,8-tetrahydroxyantraquinone, and rubicins) are also able to inhibit tau protein aggregation and even to dissolve preformed aggregates, precluding neurofibrillary tangle formation in AD.[19] Other anthraquinones substituted with (ω-*tert*-amino)-acylamino chains, such as 2,7-bis[(3-*tert*-aminopropionyl)amino]anthraquinones (**J**), exhibit high cytotoxicity against a panel of human cancer cell lines, by specifically targeting G-quadruplex and inhibiting telomerase.[20] The association of telomerase shortening and cellular senescence is well demonstrated in vitro and evidence is growing for such an association also in vivo.[21] Telomerase knockout mice exhibit decreased neurogenesis, loss of neurons, and short-term memory deficit. On the contrary, in aging APP23 transgenic mice, telomerase shortening has been shown to decrease the progression of amyloid plaque pathology and improve spatial learning ability.[22]

Very recently hybrid compounds, bearing naphtoquinone (**K**)[23] or anthraquinone(rhein) moieties (**L**, **M**)[24,25] linked to the well-known ChE inhibitors tacrine or huprine, have been reported as promising disease-modifying anti-Alzheimer drug candidates.

Based on these premises, we have now combined structural features of the previously studied ChE inhibitors[4] with those of thioxanthenone and quinoid derivatives in an attempt to obtain "single entity multitarget" agents of potential interest in the treatment of AD. The entire set of studied compounds is represented in Figure 2.

Results and discussion

Chemistry

In most of the compounds shown in Figure 2, a quinolizidine ring is linked to an aromatic amino group through a polymethylene chain of variable length. The effect of the length of the linker on biological activities has been explored on the basis of previous findings of ours and others,[5d,26–28] coming from the study from homo- and hetero-dimeric dual binding site ChE inhibitors. The optimal distance between the two moieties, interacting at the catalytic site and PAS, was attributed to the presence of 6–8 methylenes tethering the two moieties. The elongation of the spacer between the quinolizidine ring and the ar-

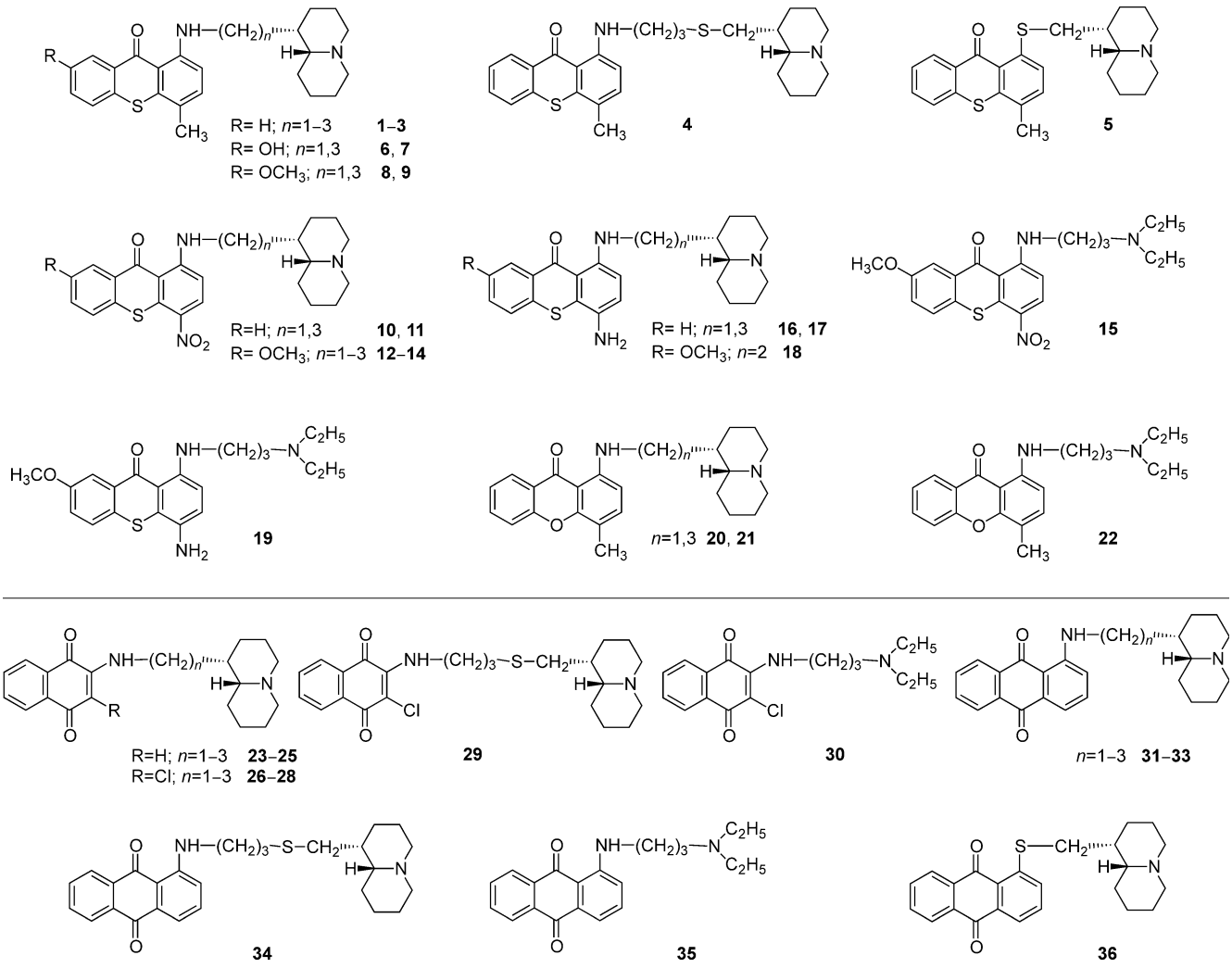

Figure 2. Thioxanthenone and xanthenone derivatives (top), and naphtho- and anthraquinone derivatives (bottom) evaluated here.

© 0000 Wiley-VCH Verlag GmbH & Co. KGaA, Weinheim

omatic system requires the preparation of long chain ω-(quinolizidin-1-yl)alkylamines. However, for compounds with more than 3 methylenes, the synthesis can be time consuming and we resorted to the use of ω-{[(quinolizidin-1-yl)methyl]thio}alkylamines, taking into account the well-known bioisosterism of a CH_2 unit to an S atom.

Twenty of the evaluated compounds have already been described by some of us (**1**–**3**, **6**–**11**, **16**, **17**;[29] **23**–**28**, **31**–**33**[30]) and assayed as antileukemic[29,30] and antimicrobial agents.[31] Compound **30** was previously described by Elslager et al.[32] The fifteen novel compounds (**4**, **5**, **12**–**15**, **18**–**22**, **29**, **34**–**36**) were prepared with the same methods used for the preparation of the known compounds, with minor modifications. Thus, for the synthesis of compounds **4** and **5**, the 1-chloro-4-methylthioxanthen-9-one[33] was reacted with 3-{[(1*R*,9a*R*)-(octahydro-2*H*-quinolizin-1-yl)methyl]thio}propan-1-amine[34] or (1*R*,9a*R*)-(octahydro-2*H*-quinolizin-1-yl)methanthiole (thiolupinine)[35] in Dowtherm A in the presence of Cs_2CO_3 (Scheme 1; Top). 1-Chloro-4-methylxanthen-9-one, prepared according to,[7a] was reacted with the suitable quinolizidinylalkylamine[36] or *N*,*N*-diethyl-1,3-propylenediamine to give **20**–**22** (Scheme 1; Bottom).

For the synthesis of compounds **12**–**15**, it was necessary to first prepare 1-chloro-7-methoxy-4-nitrothioxanthen-9-one[37] by reacting 4-methoxythiophenol with 2,6-dichloro-3-nitrobenzoic acid and then forming the thioxanthenone ring by refluxing the formed diphenyl thioether with trifluoroacetic acid and trifluoroacetic anhydride. Finally the side chains were introduced, as usual, by reacting the obtained chlorothioxanthenone with the quinolizidinylalkylamines[36] or *N*,*N*-diethyl-1,3-propylenediamine (Scheme 1; Bottom).

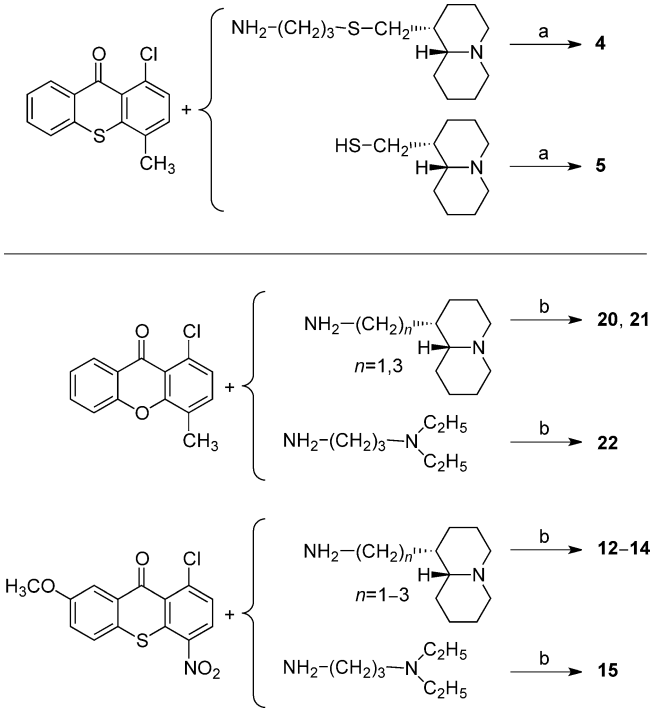

Scheme 1. *Reagents and conditions*: a) Dowtherm A, Cs_2CO_3, 170 °C, 5 h; b) chloro compound/amine (1:2), 170 °C, 6 h.

The nitro compounds **13** and **15** were reduced, in ethanol solution, with $SnCl_2$ and concd HCl to the corresponding amino compounds **18** and **19** (Scheme 2; Top). 2,3-Dichloro-1,4-naphthoquinone and 1-chloro-9,10-anthraquinone were heated with 3-{[(1*R*,9a*R*)-(octahydro-2*H*-quinolizin-1-yl)methyl]thio}propan-1-amine,[34] or *N*,*N*-diethyl-1,3-propylenediamine, or (1*R*,9a*R*)-(octahydro-2*H*-quinolizin-1-yl)methanthiole (thiolupinine)[35] to obtain the naphthoquinone **29** and the anthraquinones **34**–**36** (Scheme 2; Bottom).

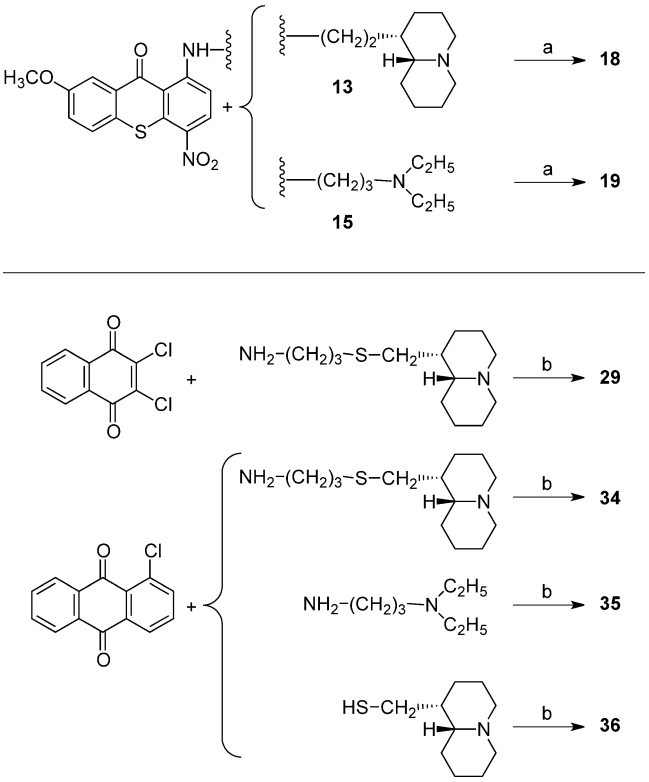

Scheme 2. *Reagents and conditions*: a) $SnCl_2$, concd HCl, EtOH, reflux 6 h; b) chloro compound/amine (1:1), 170 °C, 6 h.

Biological evaluation

Inhibitory activities on AChE (either from electric eel or recombinant human) and BChE (from equine serum) were determined by the spectrophotometric method of Ellman[38] and are reported in Tables 1 and 2 as IC_{50} values for the most active compounds or as percent inhibition at 10 μM for less active (i.e., $<50\%$) compounds.

In vitro inhibition of Aβ(1–40) aggregation was assessed following a previously reported thioflavin T (ThT) fluorescence-based method involving the use of hexafluoroisopropanol (HFIP) as aggregation enhancer.[39] For the most active compounds ($\geq 80\%$ Aβ aggregation inhibition) IC_{50} values were determined under the same assay conditions as already described;[39] data are reported in Table 1. In order to confirm the activity of these new classes of compounds, compound **2** was tested for its inhibitory activity also on Aβ(1–42) aggregation.

© 0000 Wiley-VCH Verlag GmbH & Co. KGaA, Weinheim

Table 1. Inhibitory activities of lucanthone and compounds **1**–**36** against electric eel acetylcholinesterase (eeAChE), horse serum butyrylcholinesterase (hsBChE), and Aβ aggregation.[a]

Compd	eeAChE		hsBChE		Aβ aggregation	
	Inhib. [%][b]	IC_{50} [μM]	Inhib. [%][b]	IC_{50} [μM]	Inhib. [%][b]	IC_{50} [μM]
Lucanthone	–	5.7	–	0.72	–	24
1	34	–	–	6.1	–	28
2	–	5.2	–	0.46	–	0.84
3	–	8.3	–	0.93	–	4.3
4	–	0.18	–	0.088	–	4.3
5	–	0.82	–	0.57	46	–
6	–	5.8	–	1.9	–	5.9
7	–	4.9	–	0.72	–	2.9
8	–	7.6	–	0.94	–	4.3
9	–	4.5	–	0.43	–	2.5
10	–	3.3	–	0.30	–	20
11	–	1.1	–	0.98	–	13
12	–	0.77	–	0.60	–	11
13	–	2.0	–	0.15	–	9.1
14	–	0.12	–	2.0	–	7.9
15	–	0.5	–	0.88	–	17
16	–	4.8	–	0.41	–	14
17	–	2.0	–	0.48	–	1.3
18	–	1.9	–	0.15	–	13
19	–	4.8	–	0.45	–	21
20	–	2.7	–	2.4	–	48
21	–	0.14	–	0.37	–	13
22	–	9.4	–	0.75	55	–
23	–	5.8	36	–	27	–
24	–	0.46	25	–	35	–
25	–	0.16	–	7.5	9	–
26	–	1.5	47	–	0	–
27	–	0.93	–	9.8	44	–
28	–	0.011	–	12	43	–
29	–	0.41	–	4.1	–	61
30	–	2.5	18	–	47	–
31	–	1.3	–	2.9	–	6.4
32	–	1.9	–	1.6	–	31
33	–	0.84	–	1.3	–	9.7
34	–	0.84	–	1.1	–	8.3
35	–	1.9	–	1.6	66	–
36	–	3.8	–	3.4	–	61
Donepezil	–	0.020	–	1.9	0	–
Quercetin	9	–	0	–	–	0.82

[a] Values represent the mean of two/three independent experiments; SEM always $< 10\%$. [b] % Inhibition at 10 μM (eeAChE and hsBChE) or 100 μM (Aβ aggregation).

Transmission electron microscopy (TEM) and circular dichroism (CD) spectroscopy

Aggregation kinetics were followed simultaneously for a free incubation sample of Aβ(1–40), 50 μM, and a co-incubated sample with the most active inhibitor **2** at 25 μM concentration. Incubation conditions were slightly modified from those used in the screening assay, in order to achieve a slow and complete Aβ aggregation within seven days, avoiding the use of HFIP, in phosphate-buffered saline (PBS) at the temperature of 37 °C. Dimethylsulfoxide (DMSO) was replaced with ethanol as the co-solvent (5% *v/v*).

TEM analysis was performed at 48000-fold magnification for samples of co-incubated Aβ(1–40) (50 μM) with compound **2** (25 μM), compared with a reference free incubation sample of Aβ. CD spectra were recorded in the spectral range 195–250 nm, following the conformational random coil to β-sheet transition as revealed by the increase of the negative peak of CD signal at 217 nm.

Structure-activity relationships of ChEs and Aβ aggregation inhibition

The inhibitory activities of lucanthone and compounds **1**–**36** toward AChE, BChE and Aβ(1–40) aggregation are listed in Table 1, together with those of donepezil[40] and quercetin[41] used as reference compounds. Typical dose–response curves are reported for compound **2** in Figure 3.

As a common option in the screening of small chemical libraries of Aβ aggregation inhibitors, we decided to use Aβ(1–40) instead of the more toxic and aggregation-prone Aβ(1–42). To confirm the results reported in Table 1, we also decided to test the derivative **2** in the inhibition of Aβ(1–42) aggregation, obtaining the same inhibitory response (Figure 5 b).

All tested compounds exhibited interesting inhibitory potencies on both AChE and BChE. The IC_{50} values were in the low micromolar or sub-micromolar range for at least one enzyme, but often for both of them. It is worth noting that two compounds even reached nanomolar potency: the long side chain thioxanthenone derivative **4**, which exhibited an IC_{50} for BChE = 88 nM, and the naphthoquinone derivative **28**, showing an IC_{50} for AChE = 11 nM, which was comparable to or even more potent than donepezil (IC_{50} = 20 nM; for rat brain AChE: IC_{50} = 6.7 nM[40]). Along with the most potent Aβ inhibitor **2**, compound **28** was also tested on human AChE (hAChE), and inhibitory potencies (reported in Table 2) were in the activity range determined for eeAChE.

Evaluation of inhibition kinetics of **28** on hAChE indicated a reversible, mixed-mode type, as expected for dual binding site inhibitors of AChE,[42] with a K_i value equal to 0.116 μM (Figure 4).

Indeed, all the tricyclic thioxanthenone derivatives are dual, though generally BChE-preferring inhibitors (with the excep-

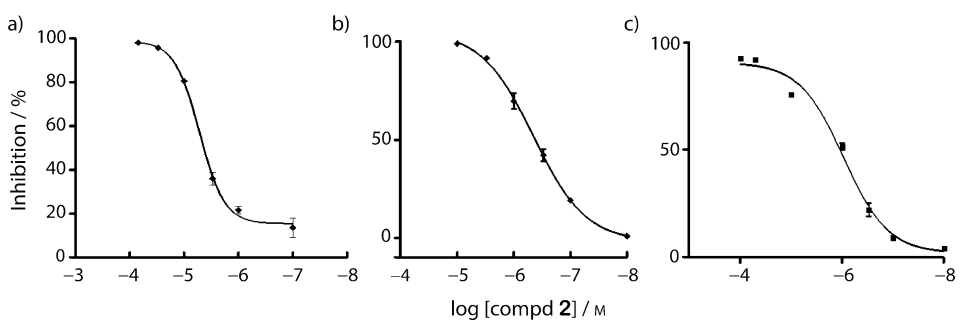

Figure 3. Inhibition dose–response curves for compound **2** against a) AChE, b) BChE, and c) Aβ(1–40).

© 0000 Wiley-VCH Verlag GmbH & Co. KGaA, Weinheim

These are not the final page numbers! ↗↗

Table 2. Inhibitory activities of compounds **2** and **28** against human acetylcholinesterase (hAChE).[a]

Compd	IC_{50} [μM]
2	3.5 ± 0.1
28	0.040 ± 0.006
Donepezil	0.019 ± 0.005

[a] Values represent the mean ± SEM of two independent experiments.

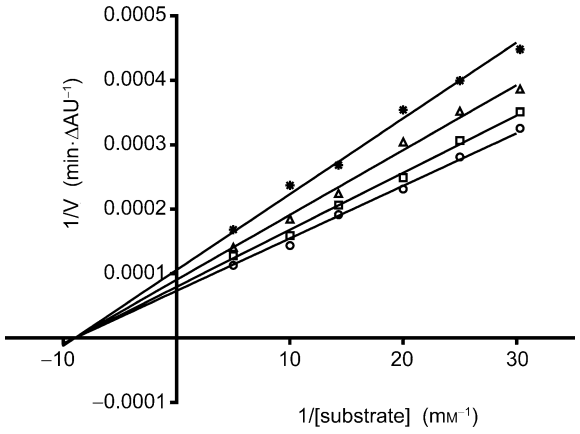

Figure 4. Lineweaver–Burk plot of inhibition kinetics of compound **28**: reciprocals of enzyme activity (hAChE) versus reciprocals of substrate (*S*-acetylthiocholine) concentration in the presence of different concentrations of inhibitor: 0 μM (○); 15 μM (□); 30 μM (△); 50 μM (*).

tion of compounds **14** and **15**), while the naphthoquinone derivatives are dual AChE-preferring inhibitors, reaching a 1000-fold selectivity in cited compound **28**. The tricyclic anthraquinone derivatives exhibited a balanced dual inhibitory activity, with an alternant slight preference for AChE or BChE.

At a concentration of 100 μM all compounds, except **25** and **26**, significantly inhibited the aggregation of Aβ. More importantly, 24 of the 37 compounds evaluated displayed IC_{50} values in the range of 0.84–31 μM, with a mean value of 11.4 μM. Of these compounds, one, four, and nineteen were xanthenone, anthraquinone, and thioxanthenone derivatives, respectively.

The 10 compounds for which it was not possible to calculate the IC_{50} (seven are naphthoquinone derivatives), still inhibited Aβ aggregation by 27–66% at a 100 μM concentration. Again, the size of the aromatic substructures (tri- versus bicyclic ring system) seems to have a greater influence on the biological activity than their chemical nature. It is worth noting that compound **2** exhibited a potency (IC_{50} = 0.84 μM) close to that of quercetin (IC_{50} = 0.82 μM), a reference anti-amyloidogenic compound.

The inhibition of Aβ aggregation is commonly associated (lucanthone and compounds **2**–**4**, **6**–**21**, **29**, **31**–**34** and **36**) with the simultaneous elevated inhibition of AChE and BChE, the latter of which is generally higher than the former (20 of 26 compounds). Moderate inhibition of Aβ aggregation was still observed for compound **1**, even if only the BChE was moderately inhibited (IC_{50} = 6.1 μM) compared to AChE (34% inhibition at 10 μM).

In contrast, when AChE inhibition (IC_{50} = 0.011–5.8 μM) largely prevailed over BChE inhibition (affinity ratio: 10–1000), as observed for naphthoquinones (**23**–**30**), Aβ aggregation was poorly inhibited or not affected at all. Two compounds (**5** and **22**) endowed with dual ChE inhibition, and specifically with sub-micromolar IC_{50} for BChE inhibition, were poorly active against Aβ aggregation (46% and 55% inhibition, respectively, at 100 μM), indicating that other factors play a role in determining this biological activity. However, it is important to emphasize that some of the presently studied compounds inhibited the ChEs and Aβ aggregation with relatively close potencies, which is a basic requisite for the potential development of therapeutic agents exhibiting multitarget activity. Thus, the most relevant inhibitors compared favorably with the reference compounds donepezil and quercetin, which are among the most potent compounds for the inhibition of ChEs and Aβ aggregation, respectively. Donepezil, a more potent AChE inhibitor than BChE, is practically devoid of inhibitory activity on direct Aβ aggregation, whereas a weak inhibition resulted from its binding at the PAS of AChE (22% inhibition at 100 μM).[43] On the other hand, quercetin (to which some of the thioxanthenone derivatives are comparable in potency as Aβ aggregation inhibitors) was inactive as a ChE inhibitor (Table 1).

Concerning further aspects of structure-activity relationships, it has already been observed that the tricyclic compounds (thioxanthenone, xanthenone, and anthraquinone derivatives) exhibited rather close patterns of biological activity (dual, but BChE-preferring, and Aβ aggregation inhibitory activities). In particular, anthraquinone derivatives resembled the thioxanthenone and xanthenone derivatives more than the chemically similar, but smaller, bicyclic naphthoquinone derivatives, which exhibited dual, but AChE-preferring inhibitory activity and quite modest activity on Aβ aggregation. The tricyclic (hetero)-aromatics are most likely capable of establishing stronger hydrophobic, π–π stacking and electrostatic interactions with the sequence of amino acids $H_{14}QKLVFF_{20}$ of Aβ, with the highest propensity to aggregate,[44] than the bicyclic system. The same tricyclic systems seemed to guarantee better interactions at the external site of BChE than on the PAS of AChE.

Within the subset of tricyclic compounds, it was important to define the influence of the sulfur bridge that differentiates the thioxanthenone derivatives from the isosteric xanthenones. It is worth noting that a number of natural[45,46] and synthetic[47–49] xanthenone derivatives have been shown to possess potent ChE inhibitory activity. However, all of them are characterized by the presence of several hydroxyl/methoxy groups or even carbamic ester function, and therefore are not directly comparable with lucanthone and the thioxanthenone derivatives considered herein. The comparison of compounds **1**, **3** and **C** (lucanthone) with the corresponding compounds **20**–**22** indicated that the sulfur bridge consistently enhances the inhibition of Aβ aggregation, while the oxygen bridge seems more suited to the inhibition of ChEs, particularly AChE.

The compounds bearing quinolizidine moieties generally display higher activities than the open dialkylaminoalkyl analogues (compare the following groups of compounds: **1**–**4** vs.

© 0000 Wiley-VCH Verlag GmbH & Co. KGaA, Weinheim

C; **12**–**14** vs. **15**; **18** vs. **19**; **20**; **21** vs. **22**; **26**–**29** vs. **30** and **31**–**34** vs. **35**). The few exceptions to such a trend mainly regard AChE and, more occasionally, BChE inhibition, suggesting that other dialkylaminoalkyl chains might give rise to more valuable activities in ChE inhibition. On the other hand, the bulky and highly lipophilic quinolizidine moiety appears particularly suited to promote the inhibition of Aβ aggregation, besides that of the ChEs.

Among the thioxanthenone and xanthenone derivatives it has been observed that the increase of the length of the linker between the 1-amino group and the quinolizidine nucleus produced an increase in activity. Examples of the few exceptions to this trend are represented by the greater BChE inhibition by 4-nitro-1-(quinolizidinylmethylamino)thioxanthenone **10** (IC_{50} = 0.3 μM) versus 1-(quinolizidinylpropylamino) homolog **11** (IC_{50} = 0.98 μM) and, more so, by the higher inhibition of Aβ aggregation by 4-methyl-1-(quinolizidinylethylamino)thioxanthenone (**2**, IC_{50} = 0.84 μM) compared to homologs **3** and **4** (IC_{50} = 4.3 μM). In addition, among the quinone compounds the polymethylene linker elongation tended to enhance the potencies of ChE inhibition. However, a remarkable 37-fold reduction of AChE inhibition was observed when the tri-methylene linker of **28** (IC_{50} = 0.011 μM) was further elongated (**29**, IC_{50} = 0.41 μM).

Concerning the inhibition of Aβ aggregation, the increasing length of the linker in the anthraquinone derivatives **31**, **33**, and **34** (1→3→5 atoms, respectively), produced only a moderate effect (IC_{50} = 6.4, 9.7, and 8.3 μM, respectively), whereas an unexpected net reduction of potency was observed when the linker was constituted of two methylene groups (**32**, IC_{50} = 31 μM).

The nature of the substituent in position 4 of the thioxanthenone ring is important for biological activity. 4-Nitro and 4-amino are less favorable substituents than 4-methyl for ChE inhibitory activity, while the influence is somewhat more variable when Aβ aggregation is accounted for. The additional presence of a 7-methoxy group often improves the activity, though several exceptions have been observed. The introduction of a chlorine atom to the naphthoquinone derivatives (**26**–**29**) clearly enhanced the potency of ChE inhibition, while its effect on Aβ aggregation was rather modest.

Finally, the exchange of the imino group on position 1 of thioxanthenone for a sulfur bridge (compare **1** with **5**) improved the inhibitory activity on the ChEs. However, this effect did not hold for Aβ aggregation. The same structural modification in anthraquinone derivatives consistently produced negative effects (compare **31** with **36**).

Kinetic studies of Aβ aggregation

The inhibitory behavior of compound **2** in the Aβ(1–40) aggregation cascade was investigated by means of CD spectroscopy, ThT fluorescence spectroscopy and TEM analysis of aggregates. Aliquots from a co-incubated sample of Aβ (50 μM) and **2** (25 μM) in PBS containing 5% ethanol were collected and analyzed over seven days of incubation at 37 °C. A free incubation sample of Aβ was used as reference. Besides its inhibitory potency (0.84 μM, that is, very similar to that of quercetin), compound **2** was also selected for its reasonable solubility, since it emerged among the most potent inhibitors (Table 1) as the most soluble in the assay medium in a preliminary UV-based solubility screening (data not shown).

The ThT fluorescence data (Figure 5a) revealed a net effect of **2** in Aβ(1–40) fibrillization, with a massive inhibition of the final fibril content. The time course of aggregation exhibited the typical sigmoidal shape, with an exponential growth of ThT fluorescence between days 1 and 3, whereas the co-incubated sample revealed a similar, though considerably flattened, sigmoidal shape. The apparent difference in inhibitory potency of **2** (80% of inhibition of ThT fluorescence at 25 μM concentration) might be compatible with its sub-micromolar IC_{50} value since incubation conditions for the time course experiment were significantly different from those used in the preliminary screening.

To confirm the antifibrillogenic effect of **2**, we performed the same ThT fluorescence experiment with Aβ(1–42) under the same assay conditions (Figure 5b). Because the aggregating propensity of Aβ(1–42) is substantially higher than Aβ(1–40), we detected a sudden increase of fluorescence in the first 24 h for the free incubation sample, with the loss of the initial lag phase. Co-incubation with **2** resulted also in a strong decrease of fluorescence that reached only 20% of the control value.

CD spectra outlined a net β-sheet arrangement for both Aβ(1–40) free and Aβ/**2** co-incubated samples, reaching almost

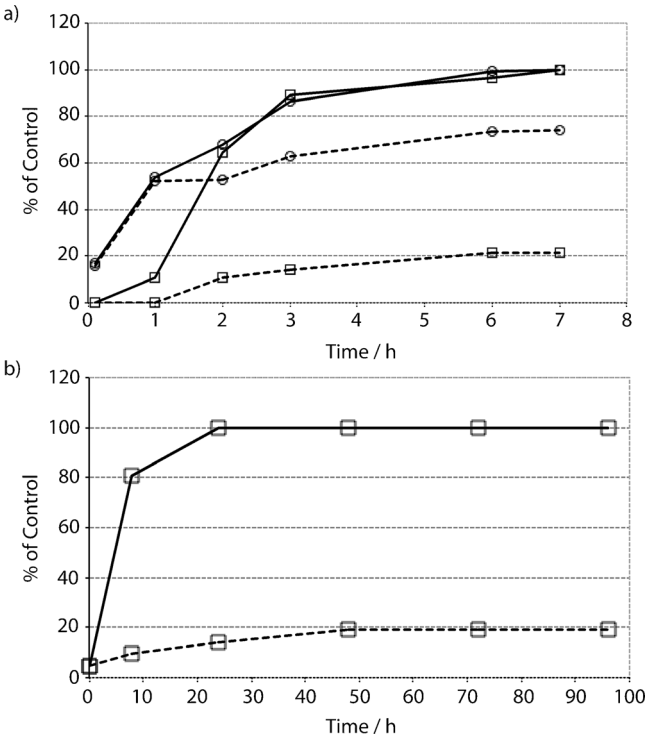

Figure 5. Typical time-course experiment of a) aggregation kinetics of Aβ(1–40) and b) Aβ(1–42). Controls (solid lines) and co-incubated with 25 μM **2** (dotted lines) in PBS/5% ethanol at 37 °C. Squares and circles represent ThT fluorescence and CD ellipticity at 217 nm, respectively. Data are expressed as a percent of maximal values obtained from controls.

© 0000 Wiley-VCH Verlag GmbH & Co. KGaA, Weinheim

60% of the final β-sheet content in the first 2 days of incubation, as shown by the negative ellipticity band centered at 217 nm. CD spectra (not reported) of both samples accounted for a stepwise rearrangement of the secondary structure from initial random coil to final β-sheet, with a small difference for co-incubated Aβ/**2**, displaying a residual content of random coil structure and a lower (80%) intensity of the β-sheet band. These data demonstrate that the antifibrillogenic activity displayed by this class of compounds is not related to the inhibition of the β-sheet arrangement, but rather to a different mechanism that we investigated by means of TEM to obtain visual proof of the shape and dimension of eventual aggregates.

The evolution of fibril formation for the same samples described above was detected at three time points: i.e., at the start (day 0), the third, and finally seventh day of incubation (Figure 6). Samples at day 0 were homogeneously devoid of any prefibrillar aggregate, both in the control (Figure 6a) and in the co-incubated sample (Figure 6d). At day 3, a network of fibrillar species was already visible in both control and co-incubated specimens (Figures 6b,e), leading at day 7 to the massive formation of tangles (Figures 6c,f). The amount of fibrillar species formed also in the presence of **2** suggested that the quenching of ThT fluorescence cannot be explained by the mere inhibition of fibril formation, but rather with a different structural arrangement that hampers ThT staining.

For a sound explanation of these results, a statistical analysis was performed to determine the average diameter of fibrils formed at 3 and 7 days of incubation for both the control (d) and co-incubated (d') samples. At day 3, average d and d' were 13.3 ± 2.4 nm and 10.5 ± 2.3 nm, respectively. At day 7, the thickness of control fibrils slightly increased to 13.8 ± 3.1 nm, while for the co-incubated sample it was 9.4 ± 1.7 nm. Such average diameters are fully compatible with those reported in the literature;[50] worthy of note is the difference of approximately 4 nm between d and d' of fibrils finally formed after 7 days. Visual inspection revealed that the fibrillar structures formed in the presence of the inhibitor appeared at all times to be more rigid, inhomogeneous and to curl compared to those of the control specimen. The loss of ThT staining could therefore be ascribed to a destabilizing effect of the inhibitor in the correct evolution and assembly of prefibrillar species into mature fibrils.

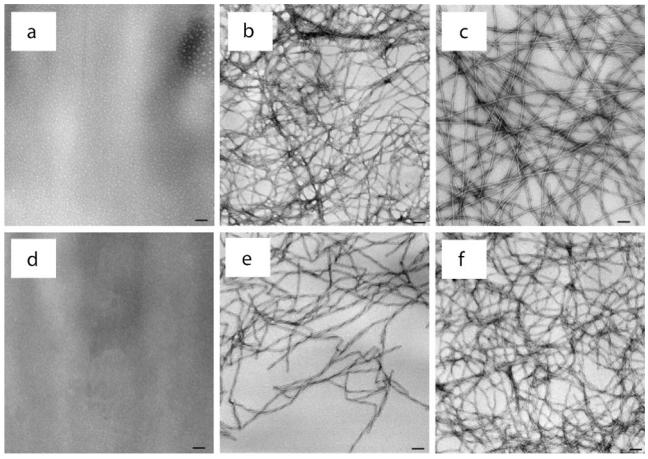

Figure 6. Transmission electron microscopy (TEM) micrographs of samples from aggregation kinetics of 50 μM Aβ(1–40) alone (a–c) or co-incubated with 25 μM **2** (d–f) in PBS/5% ethanol at 37 °C. Samples were collected at time point zero (a,d), 3 (b,e) and 7 (c,f) days of incubation. Scale bars: 100 nm.

In vitro blood–brain barrier (BBB) permeability assays

Even if all tested compounds have molecular weight lower than 500 Da and log D from 2 to 4 (ACDLabs, software V11.02), which should not challenge their ability to cross cell membranes, two compounds (**2** and **28**) representative of thioxanthenone and naphthoquinone subsets of compounds, were investigated for their ability to permeate, by passive diffusion, the BBB and to interact with P-glycoprotein (P-gp), which plays an important role in the efflux transport of drugs. To this purpose, transport studies involving these compounds were performed on Madin–Darby canine kidney cells retrovirally transfected with human multidrug resistance gene 1 (MDCKII-MDR1), which are characterized by a high expression of P-gp, and represent a well-established in vitro method to mimic the BBB.[51,52] Transport studies were conducted both in apical (AP) to basolateral (BL) and BL to AP direction and results are reported in Table 3.

Compounds **2** and **28** showed efflux ratio (ER) equal to 0.95 and 0.78, respectively, suggesting that they are able to permeate the monolayer with permeability at least comparable to diazepam (ER = 0.79).

Table 3. Bidirectional transport across MDCKII-MDR1 cells of compounds **2** and **28**.

Compd	P_{app} [cm sec^{-1}][a]		ER[b]
	AP→BL	BL→AP	(BL/AP)
2	6.40×10^{-5}	6.08×10^{-5}	0.95
28	3.02×10^{-5}	2.35×10^{-5}	0.78
Diazepam	1.56×10^{-5}	1.23×10^{-5}	0.79
FD4[c]	1.13×10^{-6}	2.68×10^{-7}	0.23

[a] Apical to basolateral (AP→BL) and basolateral to apical (BL→AP) permeability (P_{app}). [b] Efflux ratio (ER) was calculated using the following equation: $ER = P_{app}(BL)/P_{app}(AP)$; for details, see Experimental Section. [c] Fluorescein isothiocyanate-dextran (FD4).

Cytotoxicity assays

The assessment of safety profile is fundamental for drugs intended for use over a prolonged period of time, as is the case for AD treatment. To achieve a preliminary assessment of the neurotoxicity of the studied compounds, cytotoxicity assays were carried out against the human neuroblastoma cell line SH-SY5Y, commonly used in neurobiological studies. Compounds **2** and **28** were selected for evaluation as representatives of the thioxanthenone and naphthoquinone subsets of compounds, respectively. Thioxanthenone **2** was the most potent inhibitor of Aβ aggregation, while naphthoquinone **28** was the most potent inhibitor of AChE.

© 0000 Wiley-VCH Verlag GmbH & Co. KGaA, Weinheim

Table 4. Cytotoxicity and inhibitory activities of compounds **2** and **28**.

Compd	IC_{50} [μM]				Selectivity ratio		
	tox[a]	AChE[b]	BChE[b]	Aβ agg.[b]	(Tox/AChE)	(Tox/BChE)	(Tox/Aβ)
2	7.2 ± 0.1	5.2	0.46	0.84	1.38	15.65	8.52
28	3.6 ± 0.2	0.011	12	–	327	0.3	–

[a] Test compound concentration required to induce 50% cell survival inhibition against human neuroblastoma cell line SH-SY5Y in vitro after 24 h of incubation; values represent the mean ± SEM of two independent experiments performed in duplicate. [b] Values represent the mean of two/three independent experiments; SEM always < 10%. [c] Selectivity ratio: IC_{50}(SH-SY5Y)/IC_{50}(ChE or Aβ).

As shown in Table 4 they had a comparable cytotoxicity effect after 24 h of incubation, with IC_{50} values of 7.2 ± 0.1 μM and 3.6 ± 0.2 μM, respectively. For compound **28**, the IC_{50} value for cytotoxicity was 327-fold higher than the IC_{50} value for AChE inhibition. However, on the whole, the results of Table 4 indicate a rather narrow safety margin.

On the other hand, based on the results of the testing for antileukemic activity,[29,30] only a low-to-moderate level of in vivo toxicity is expected for the present compounds. Indeed, no mortality was observed when several of these compounds were injected i.p. at the dose of 50–200 mg kg^{-1}, once a day for five consecutive days, in a group of six mice, which had been previously inoculated with leukemia P388 cells. Compound **1** (the lower homologue of **2**) at a dose of 200 mg kg^{-1} for nine days prolonged the mouse survival time by 24%; thus its i.p. LD_{50} value should be quite superior to the indicated dosage. Donepezil and galantamine, two current drugs for AD, have been shown to exhibit higher toxicity in mice, with oral LD_{50} equal to 45 and 18.7 mg kg^{-1}, respectively.[53,54]

For a more meaningful assessment of the value of the present compounds, the issue of their in vitro and in vivo toxicity, in comparison to established drugs for AD, should be further investigated.

Conclusions

Based on the models of compounds previously described as capable of maintaining or restoring cell protein homeostasis and of inhibiting Aβ oligomerization, 37 thioxanthen-9-one, xanthen-9-one, naphtho- and anthraquinone derivatives were tested for the direct inhibition of Aβ aggregation and the inhibition of AChE and BChE. These compounds are characterized by the presence of basic side chains, mainly quinolizidinylalkyl moieties, that have been recently shown to produce potent ChE inhibitors when linked to various bi- and tri-cyclic (hetero)aromatic systems.[4]

With very few exceptions, all these compounds were able to display inhibitory activity on both AChE and BChE and on the spontaneous aggregation of Aβ. In this regard, the time course of amyloid aggregation in the presence of **2** revealed that these compounds might act as destabilizers of mature fibrils rather than mere inhibitors of fibrillization. Their potential utility in the control of symptoms and/or progression of AD would therefore be confirmed only after an extensive biophysical evaluation of prefibrillar, oligomeric species (i.e., the true neurotoxic species of Aβ).

Most compounds exhibited IC_{50} values in the low micromolar or sub-micromolar range for the different biological activities. Some compounds even reached nanomolar potency; for example, thioxanthenone derivative **4**, with an IC_{50} value of 88 nM for the inhibition of BChE, and chloronaphthoquinone derivative **28** with an IC_{50} value of 11 nM for AChE inhibition.

More importantly, many compounds inhibited one or both ChEs and Aβ aggregation with similar potencies, thus fulfilling a fundamental requirement for a multitarget mechanism of action. Among these compounds, the thioxanthenone derivatives **2**, **4**, **7**, and **9**, and most of all **17**, as well as anthraquinones **33** and **34** warrant further investigation.

Exploratory investigations on compounds **2** and **28**, as representative of the thioxanthenone and naphthoquinone subsets of compounds, have indicated that they might penetrate the BBB with a permeability comparable or even superior to that of diazepam.

In vitro assays for cytotoxicity against the neuroblastoma cell line SH-SY5Y indicated a rather narrow safety margin for the two compounds evaluated, which is somewhat conflicting with the low-to-moderate in vivo toxicity previously observed.[29,30] Thus, this issue deserves further investigations in order to establish the value of the present compounds as potential agents for the treatment of AD.

Experimental Section

Chemistry

General: Chemicals, solvents and reagents used for the syntheses were purchased from Sigma–Aldrich, Fluka or Alfa Aesar, and were used without any further purification. Column chromatography (CC): neutral alumina (Al_2O_3), activity 1 (Merck). Mps: Büchi apparatus, uncorrected. ^{1}H NMR and ^{13}C NMR spectra: Bruker Avance DPX-300 or Varian Gemini-200 spectrometers; $CDCl_3$; δ in ppm rel. to Me_4Si as internal standard. *J* in Hz. Elemental analyses were performed on a Carlo Erba EA-1110 CHNS-O instrument in the Microanalysis Laboratory of the Department of Pharmacy of Genoa University.

General procedure for the synthesis of compounds 4, 5, 12–15, 20–22, 29 and 34–36: A mixture of the suitable reactive chloro derivative (1-chloro-4-methyl-9*H*-xanthen-9-one; 1-chloro-7-methoxy-4-nitro-9*H*-thioxanthen-9-one; 2,3-dichloro-1,4-naphthoquinone; 1-chloro-9,10-anthraquinone) with the suitable amino compound [(1*S*,9a*R*)-(octahydro-2*H*-quinolizin-1-yl)alkylamines;[36] 3-{[(1*R*,9a*R*)-(octahydro-2*H*-quinolizin-1-yl)methyl]thio}propan-1-amine;[34] (1*R*,9a*R*)-(octahydro-2*H*-quinolizin-1-yl)methanthiole (thiolupinine);[35] *N*,*N*-diethyl-1,3-propylenediamine] was heated at 170 °C in a closed tube for 6 h. The ratio between chloro compound/amine was 1:2 for compounds **12**–**15** and **20**–**22**, and was 1:1 for compounds **29** and **34**–**36**.

© 0000 Wiley-VCH Verlag GmbH & Co. KGaA, Weinheim

To synthesize compounds **4** and **5**, 1-chloro-4-methyl-9*H*-thioxanthen-9-one (2.3 mmol) was reacted with 3-{[(1*R*,9a*R*)-(octahydro-2*H*-quinolizin-1-yl)methyl]thio}propan-1-amine or thiolupinine in a ratio 1:1 and in solution of Dowtherm A (2 mL) and in the presence of Cs_2CO_3 (2.3 mmol), heating at 170 °C for 5 h.

1-Chloro-4-methyl-9*H*-xanthen-9-one and 1-chloro-4-methyl-9*H*-thioxanthen-9-one were used as mixtures with the unreactive isomers as indicated in References [7a] and [33].

In all cases at r.t. the mixture was triturated with 2 N HCl and extracted with Et_2O. Then the acid solution was basified with 6 N NaOH and exhaustively extracted with Et_2O or CH_2Cl_2. The organic layer was washed with water and, after drying (Na_2SO_4), evaporated affording a residue that was crystallized from the indicated solvent or purified by CC (Al_2O_3/Et_2O or CH_2Cl_2). In the case of compounds **4**, **22**, **34** and **35** the oily residue was converted into the corresponding monohydrochloride with 1 N ethanolic solution of HCl.

4-Methyl-1-{3-[(1*R*,9a*R*)-(octahydro-2*H*-quinolizin-1-yl)methylthio]prop-1-yl-amino}-9*H*-thioxanthen-9-one (4): Oil. CC(Al_2O_3/CH_2Cl_2); yield: 43%; ^{1}H NMR (200 MHz, $CDCl_3$):δ = 0.94–2.22 (m, 16H, 14H of Q and 2H of $CH_2CH_2CH_2$), 2.36 (s, CH_3-Ar), 2.62–2.99 (m, 6H, 2Hα near N of Q, 2H of $CH_2CH_2CH_2$-S and 2H of SCH_2), 3.34–3.55 (m, 2H, $NHCH_2$), 6.61 (d, J = 7.6 Hz, 1H, ArH), 7.21–7.68 (m, 4H, ArH), 8.52 (dd, J = 7.6, 0.9 Hz, 1H, ArH), 10.12 ppm (s, NH, collapses with D_2O); Anal. calcd for $C_{27}H_{34}N_2OS_2$: C 69.49, H 7.34, N 6.00, S 13.74, found: C 69.71, H 7.07, N 6.28, S 13.45; monohydrochloride: mp: 152–154 °C (EtOH/Et_2O); Anal. Calcd for $C_{27}H_{34}N_2OS_2$ + HCl: C 64.45, H 7.01, N 5.57, S 12.75, found: C 64.33, H 7.09, N 5.37, S 12.00.

4-Methyl-1-{[(1*R*,9a*R*)-(octahydro-2*H*-quinolizin-1-yl)methyl]thio}-9*H*-thioxanthen-9-one (5): Yellow crystals (CH_2Cl_2); yield: 66%; mp: 113–115 °C; ^{1}H NMR (200 MHz, $CDCl_3$): δ = 1.04–2.33 (m, 14H of Q), 2.50 (s, CH_3-Ar), 2.79–3.38 (m, 4H, 2Hα near N of Q and 2H of SCH_2), 7.24–7.82 (m, 5H, ArH), 8.60 ppm (d, J = 7.6 Hz, 1H, ArH); Anal. calcd for $C_{24}H_{27}NOS_2$: C 70.38, H 6.64, N 3.42, S 15.65, found: C 70.39, H 6.67, N 3.47, S 15.26

7-Methoxy-4-nitro-1-{[(1*S*,9a*R*)-(octahydro-2*H*-quinolizin-1-yl)methyl]amino}-9*H*-thio-xanthen-9-one (12): Dark yellow crystals (Et_2O/pentane); yield: 57%; mp: 194–196 °C; ^{1}H NMR (200 MHz, $CDCl_3$): δ = 1.11–2.42 (m, 14H of Q), 2.91–3.12 (m, 2Hα near N of Q), 3.62–3.80 (m, 2H, $NHCH_2$), 3.97 (s, 3H, OCH_3), 6.78 (d, J = 9.2 Hz, 1H, ArH), 7.26–7.38 (m, 1H, ArH), 7.63 (d, J = 8.6 Hz, 1H, ArH), 7.97 (d, J = 2.8 Hz, 1H, ArH), 8.56 (d, J = 9.2 Hz, 1H, ArH), 12.03 ppm (s, NH-Ar, collapses with D_2O); ^{13}C NMR (200 MHz, $CDCl_3$): δ = 19.8, 23.8, 24.2, 26.8, 28.7, 37.3, 41.2, 54.6, 56.2, 63.6, 106.4, 108.0, 110.0, 121.6, 126.4, 127.8, 129.3, 129.4, 131.3, 141.3, 156.8, 158.2, 181.5 ppm; Anal. calcd for $C_{24}H_{27}N_3O_4S$: C 63.56, H, 6.00, N 9.26, S 7.07, found: C 63.42, H 5.96, N 9.64, S 6.85.

7-Methoxy-4-nitro-1-{[(1*S*,9a*R*)-(octahydro-2*H*-quinolizin-1-yl)-ethyl]amino}-9*H*-thioxanthen-9-one (13): Red crystals (Et_2O/pentane); yield: 67%; mp: 170–173 °C; ^{1}H NMR (300 MHz, $CDCl_3$): δ = 1.20–2.04 (m, 16H, 14H of Q and 2H of $NHCH_2CH_2$), 2.77–2.93 (m, 2Hα near N of Q), 3.22–3.48 (m, 2H, $NHCH_2CH_2$), 3.96 (s, 3H, OCH_3), 6.50 (d, J = 6.0 Hz, 1H, ArH), 7.00 (d, J = 6.0 Hz, 1H, ArH), 7.10–7.21 (m, 1H, ArH), 7.46 (d, J = 6.0 Hz, 1H, ArH), 7.98 (d, J = 2.0 Hz, 1H, ArH), 9.77 ppm (s, NH-Ar, collapses with D_2O); Anal. calcd for $C_{25}H_{29}N_3O_4S$: C 64.22, H 6.25, N 8.99, S 6.86, found: C, 64.19, H 6.42, N 8.99, S 6.49.

7-Methoxy-4-nitro-1-{[(1*S*,9a*R*)-(octahydro-2*H*-quinolizin-1-yl)prop-1-yl]amino}-9*H*-thio-xanthen-9-one (14): Dark yellow crystals (Et_2O/pentane); yield: 46%; mp: 112–114 °C; ^{1}H NMR (300 MHz, $CDCl_3$): δ = 1.12–2.18 (m, 18H, 14H of Q and 4H of $CH_2CH_2CH_2$-Q), 2.78–2.94 (m, 2Hα near N of Q), 3.28–3.45 (m, 2H, $NHCH_2$), 3.87 (s, 3H, OCH_3), 6.57 (d, J = 6.0 Hz, 1H, ArH), 7.18–7.27 (m, 1H, ArH), 7.52 (d, J = 6.0 Hz, 1H, ArH), 7.85 (d, J = 2.0 Hz, 1H, ArH), 8.44 (d, J = 6.0 Hz, 1H, ArH), 11.86 ppm (s, NH, collapses with D_2O); Anal. calcd for $C_{26}H_{31}N_3O_4S$: C 64.84, H 6.49, N 8.72, S 6.66, found: C 64.97, H 6.39, N 8.37, S 6.87.

1-{[3-(*N*,*N*-Dimethylamino)prop-1-yl]amino}-7-methoxy-4-nitro-9*H*-thioxanthen-9-one (15): Dark yellow crystals (Et_2O/pentane); yield: 66%; mp: 101–103 °C; ^{1}H NMR (200 MHz, $CDCl_3$): δ = 1.19 (t, J = 7.0 Hz, 6H, $N(CH_2CH_3)_2$), 2.00–2.24 (m, 2H, $CH_2CH_2CH_2N(C_2H_5)_2$), 2.60–2.94 (m, 6H, $CH_2CH_2CH_2N(CH_2CH_3)_2$), 3.42–3.60 (m, 2H, $NHCH_2CH_2CH_2N(C_2H_5)_2$)), 3.96 (s, 3H, OCH_3), 6.68 (d, J = 9.8 Hz, 1H, ArH), 7.20–7.32 (m, 1H, ArH), 7.57 (d, J = 8.8 Hz, 1H, ArH), 7.89 (d, J = 2.8 Hz, 1H, ArH), 8.49 (d, J = 9.8 Hz, 1H, ArH), 11.96 ppm (s, NH, collapses with D_2O); Anal. calcd for $C_{21}H_{25}N_3O_4S$: C 60.70, H 6.06, N 10.11, S 7.72, found: C 60.64, H 6.00, N 10.18, S 7.41.

4-Methyl-1-{[(1*S*,9a*R*)-(octahydro-2*H*-quinolizin-1-yl)methyl]amino}-9*H*-xanthen-9-one (20): Yellow crystals (Et_2O); yield: 67%; mp: 109–111 °C; ^{1}H NMR (200 MHz, $CDCl_3$): δ = 1.08–2.24 (m, 14H of Q), 2.36 (s, CH_3-Ar), 2.81–2.96 (m, 2Hα near N of Q), 3.30–3.60 (m, 2H of $NHCH_2$), 6.42 (d, J = 9.8 Hz, 1H, ArH), 7.24–7.72 (m, 4H, ArH), 8.24 (d, J = 9.2 Hz, 1H, ArH), 9.38 ppm (s, NH, collapses with D_2O); Anal. calcd for $C_{24}H_{28}N_2O_2$: C 76.56, H 7.50, N 7.44, found: C 76.21, H 7.38, N 7.68.

4-Methyl-1-{[(1*S*,9a*R*)-(octahydro-2*H*-quinolizin-1-yl)prop-1-yl]-amino}-9*H*-xanthen-9-one (21): Yellow crystals (Et_2O); yield: 40%; mp: 82–84 °C; ^{1}H NMR (200 MHz, $CDCl_3$): δ = 1.05–2.00 (m, 18H, 14H of Q and 4H of $CH_2CH_2CH_2$-Q), 2.37 (s, CH_3-Ar), 2.86–3.14 (m, 2Hα near N of Q), 3.18–3.36 (m, 2H, $NHCH_2$), 6.36 (d, J = 8.4 Hz, 1H, ArH), 7.23–7.74 (m, 4H, ArH), 8.24 (d, J = 7.8 Hz, 1H, ArH), 9.38 ppm (s, NH, collapses with D_2O); ^{13}C NMR (200 MHz, $CDCl_3$): δ = 13.9, 20.1, 23.9, 26.7, 27.0, 37.2, 42.3, 56.3, 64.8, 102.0, 105.8, 108.9, 116.2, 121.0, 122.3, 124.9, 132.8, 136.5, 149.3, 154.3, 154.4, 179.0 ppm; Anal. calcd for $C_{26}H_{32}N_2O_2$: C 77.19, H 7.97, N 6.92, found: C 76.95, H 8.20, N 7.05.

1-{[3-(*N*,*N*-Diethylamino)prop-1-yl]amino}-4-methyl-9*H*-xanthen-9-one (22): Oil, CC(Al_2O_3/Et_2O); yield: 58%; ^{1}H NMR (200 MHz, $CDCl_3$): δ = 1.07 (t, J = 7.4 Hz, 6H, $N(CH_2CH_3)_2$), 1.80–2.20 (m, 2H, $CH_2CH_2CH_2N(C_2H_5)_2$), 2.35 (s, CH_3-Ar), 2.40–2.78 (m, 6H, $CH_2CH_2CH_2N(CH_2CH_3)_2$), 3.17–3.39 (m, 2H, $NHCH_2CH_2CH_2N(C_2H_5)_2$)), 6.36 (d, J = 9.8 Hz, 1H, ArH), 7.20–7.71 (m, 4H, ArH), 8.23 (d, J = 9.4 Hz, 1H, ArH), 9.37 ppm (s, NH, collapses with D_2O); monohydrochloride: mp 176–179 °C (EtOH/Et_2O); Anal. Calcd for $C_{21}H_{26}N_2O_2$ + HCl: C 67.28, H 7.26, N 7.47, found: C 67.29, H 7.51, N 7.63.

3-Chloro-2-{[(1*S*,9a*R*)-(octahydro-2*H*-quinolizin-1-yl)methylthio]-prop-1-ylamino}-1,4-naphthoquinone (29): Yellow crystals, CC(Al_2O_3/CH_2Cl_2); yield: 63%; mp: 96–97 °C; ^{1}H NMR (200 MHz, $CDCl_3$): δ = 0.94–2.24 (m, 16H, 14H of Q and 2H of $CH_2CH_2CH_2S$), 2.64 (t, J = 6.4 Hz, 2H, $CH_2CH_2CH_2S$), 2.72–3.04 (m, 4H, 2Hα near N of Q and 2H of SCH_2), 3.88–4.12 (m, 2H, $NHCH_2$), 6.23 (s, NH, collapses with D_2O), 7.59–7.82 (m, 2H, ArH), 7.98–8.24 (m, 2H, ArH), 9.82 ppm (s, NH, collapses with D_2O); Anal. calcd for $C_{23}H_{29}ClN_2O_2S$: C 63.80, H, 6.75, N 6.47, S 7.41, found: C 64.10, H 6.49, N 6.42, S 7.08.

1-{3-[(1*R*,9a*R*)-(Octahydro-2*H*-quinolizin-1-yl)methylthio]prop-1-ylamino}-9,10-anthraquinone (34): Oil, CC(Al_2O_3/CH_2Cl_2); yield: 57%, ^{1}H NMR (200 MHz, $CDCl_3$): δ = 0.94–2.26 (m, 16H, 14H of Q and 2H of $CH_2CH_2CH_2$), 2.57–3.05 (m, 6H, 2Hα near N of Q, 2H of

© 0000 Wiley-VCH Verlag GmbH & Co. KGaA, Weinheim

$CH_2CH_2CH_2$-S and 2H of SCH_2), 3.38–3.62 (m, 2H, NH-$CH_2CH_2CH_2$), 7.12 (dd, J=9.2, 1.6 Hz, 1H, ArH), 7.43–7.88 (m, 4H, ArH), 8.16–8.40 (m, 2H, ArH), 9.82 ppm (s, NH, collapses with D_2O); Anal. calcd for $C_{27}H_{32}N_2O_2S$: C 72.29, H 7.19, N 6.24, S 7.15, found: C 72.03, H 6.98, N 6.47, S 7.42; monohydrochloride (hygroscopic): Anal. calcd for $C_{27}H_{32}N_2O_2S+HCl+2H_2O$: C 62.23, H 7.16, N 5.38, S 6.15, found: C 62.48, H 7.48, N 5.60, S 6.15.

1-{[3-(*N*,*N*-Dimethylamino)prop-1-yl]amino}-9,10-anthraquinone (35): Oil, CC(Al_2O_3/Et_2O); yield: 70%, ^{1}H NMR (300 MHz, $CDCl_3$): δ= 1.46 (t, J=7.4 Hz, 6H, $N(CH_2CH_3)_2$), 2.26–2.44 (m, 2H, $CH_2CH_2CH_2N(C_2H_5)_2$), 3.10–3.36 (m, 6H, $CH_2CH_2CH_2N(CH_2CH_3)_2$), 3.54 (t, J=7.4 Hz, 2H, $NHCH_2CH_2CH_2N(C_2H_5)_2$)), 7.06 (d, J=8.8 Hz, 1H, ArH), 7.52–7.81 (m, 4H, ArH), 8.22 (d, J=8.6 Hz, 2H, ArH), 12.24 ppm (s, NH, collapses with D_2O); ^{13}C NMR (200 MHz, $CDCl_3$): δ=7.5, 22.5, 24.2, 39.3, 45.7, 48.5, 112.3, 115.3, 116.7, 125.6, 131.8, 132.1, 132.9, 133.5, 133.6, 134.5, 149.9, 182.3, 184.1 ppm; monohydrochloride: mp: 224–226 °C (EtOH/Et_2O); Anal. calcd for $C_{21}H_{24}N_2O_2+HCl$: C 67.64, H 6.76, N 7.51, found: C 67.44, H 7.11, N 7.44.

1-{[(1*R*,9a*R*)-(Octahydro-2*H*-quinolizin-1-yl)methyl]thio}-9,10-anthraquinone (36): Yellow crystals (EtOH); yield: 64%, mp: 182–184 °C; ^{1}H NMR (200 MHz, $CDCl_3$): δ=0.96–2.28 (m, 14H of Q), 2.71–2.98 (m, 2Hα near N of Q), 3.06–3.21 (m, 2H of SCH_2), 7.62–7.97 (m, 4H, ArH), 8.09–8.46 ppm (m, 3H, ArH); Anal. calcd for $C_{24}H_{25}NO_2S$: C 73.62, H 6.44, N 3.58, S 8.19, found: C 73.80, H 6.06, N 3.22, S 8.01.

General procedure for the synthesis of compounds 18 and 19: To a stirred soln. of the 4-nitroderivative **13** or **15** (0.96 mmol) in EtOH (20 mL), a solution of $SnCl_2\cdot2H_2O$ (0.76 g, 3.36 mmol) in concd HCl (5 mL) was slowly added. The mixture was refluxed for 6 h and then concentrated in vacuo. The residue was taken up in H_2O, alkalized with 6 N NaOH and repeatedly extracted with Et_2O. After drying (Na_2SO_4), the solvent was removed and the oily residue converted into the dihydrochloride.

4-Amino-7-methoxy-1-{[(1*S*,9a*R*)-(octahydro-2*H*-quinolizin-1-yl)-ethyl]amino}-9*H*-thio- xanthen-9-one (18): Red oil; yield: 61%; ^{1}H NMR (300 MHz, $CDCl_3$): δ=1.10–2.06 (m, 16H, 14H of Q and 2H of $NHCH_2CH_2$), 2.75–2.90 (m, 2Hα near N of Q), 3.08–3.42 (m, 4H, 2H of $NHCH_2CH_2$ and 2H of NH_2-Ar, collapse with D_2O), 3.86 (s, 3H, OCH_3), 6.47 (d, J=6.0 Hz, 1H, ArH), 6.95 (d, J=6.0 Hz, 1H, ArH), 7.08–7.20 (m, 1H, ArH), 7.37 (d, J=6.0 Hz, 1H, ArH), 7.93 (d, J=2.0 Hz, 1H, ArH), 9.78 ppm (s, NH-Ar, collapses with D_2O); dihydrochloride: mp: 235–238 °C (EtOH); Anal. calcd for $C_{25}H_{31}N_3O_2S+2HCl$: C 58.82, H 6.52, N 8.23, S 6.28, found: C 59.10, H 6.73, N 8.08, S 6.36.

4-Amino-1-{[3-(*N*,*N*-dimethylamino)prop-1-yl]amino}-7-methoxy-9*H*-thioxanthen-9-one (19): Red oil; yield: 65%; ^{1}H NMR (200 MHz, $CDCl_3$): δ=1.19 (t, J=7.2 Hz, 6H, $N(CH_2CH_3)_2$), 1.92–2.14 (m, 2H, $CH_2CH_2CH_2N(C_2H_5)_2$), 2.57–2.98 (m, 6H, $CH_2CH_2CH_2N(CH_2CH_3)_2$), 3.22–3.56 (m, 4H, 2H of $NHCH_2CH_2CH_2N(C_2H_5)_2$ and 2H of NH_2-Ar, collapse with D_2O), 3.94 (s, 3H, OCH_3), 6.55 (d, J=8.8 Hz, 1H, ArH), 7.04 (d, J=8.8 Hz, 1H, ArH), 7.17 (dd, J=8.8, 3.0 Hz, 1H, ArH), 7.46 (d, J=8.8 Hz, 1H, ArH), 8.00 (d, J=2.8 Hz, 1H, ArH), 9.86 ppm (s, NH, collapses with D_2O); dihydrochloride: mp: 230–233 °C (EtOH); Anal. calcd for $C_{21}H_{27}N_3O_2S+2HCl$: C 55.02, H 6.38, N 9.17, S 6.99, found: C 55.20, H 6.43, N 9.08, S 7.37.

Biological methods

General: All reagents and enzymes were purchased from Sigma–Aldrich Italy, unless otherwise specified. For title compounds, the concentration required to inhibit 50% of the tested activity (IC_{50}) was determined by evaluating 5–7 concentrations in duplicate, ranging from 100 to 0.01 μM, and calculated by nonlinear regression of the response/log(concentration) curve, using GraphPad Prism v. 5.01 software (La Jolla, CA, USA). Values were obtained as the mean from two/three independent experiments.

Inhibition of cholinesterases: The in vitro inhibition assays of electric eel AChE (463 U mg^{-1}) or human recombinant AChE (2770 U mg^{-1}), and BChE from equine serum (13 U mg^{-1}) were run in phosphate buffer (0.1 M, pH 8.0). Acetyl- and butyrylthiocholine iodides were used, respectively, as substrates, and 5,5′-dithiobis(2-nitrobenzoic acid) (DTNB) was used as the chromophoric reagent.[38] Inhibition assays were carried out on an Agilent 8453E UV-visible spectrophotometer equipped with a cell changer. Solutions of tested compounds were prepared starting from 10 mM stock solutions in DMSO, which were diluted with water to a final content of organic solvent always lower than 1%. AChE inhibitory activity was determined in a reaction mixture containing AChE (100 μL, 0.9 U mL^{-1} in 0.1 M phosphate buffer, pH 8.0), DTNB (100 μL, 3.3 mM in 0.1 M phosphate buffer (pH 7.0) containing 6 mM $NaHCO_3$), inhibitor (100 μL, 6–7 concentrations from 1×10^{-8} to 1×10^{-4} M), and work buffer (600 μL). After incubation for 20 min at 25 °C, acetylthiocholine iodide (100 μL of 5 mM aqueous solution) was added as the substrate, and AChE-catalyzed hydrolysis was followed by measuring the increase of absorbance at 412 nm for 5.0 min at 25 °C. BChE inhibitory activity was assessed similarly using butyrylthiocholine iodide as the substrate.

Kinetic studies of hAChE inhibition: Kinetic studies were performed under the same incubation conditions described above, using six concentrations of substrate (0.033–0.2 mM) and four concentrations of inhibitor **28** (0–50 nM). Apparent inhibition constant and kinetic parameters were calculated within the 'Enzyme kinetics' module of Prism.

Thioflavin T fluorescence spectroscopy analysis: To obtain batches of Aβ(1–40) and Aβ(1–42) free from preaggregates, commercial peptides (purity > 95%; EzBiolab, Carmel, USA) were dissolved in hexafluoroisopropanol (HFIP), lyophilized and stored at −20 °C. The solution of thioflavin T (ThT) (25 μM) used for fluorimetric measures was prepared in phosphate buffer (0.025 M, pH 6.0, filtered through 0.45 μm nylon filters and stored at 4 °C). For Aβ(1–40) inhibition, compounds were first tested at 100 μM. Test samples were prepared in phosphate-buffered saline (PBS; 0.01 M, NaCl 0.1 M, pH 7.4), with 30 μM Aβ peptide concentration, and contained 2% HFIP and 10% DMSO. Blank samples were prepared for each concentration, devoid of peptide, and their fluorescence value subtracted from the corresponding fluorescence values of co-incubation samples. As the control, a sample of peptide was incubated in the same PBS/2% HFIP/10% DMSO buffer, without inhibitor. Incubations were run in triplicate at 25 °C for 2 h. Fluorimetric measures were performed in a 700 μL cuvette with a PerkinElmer LS55 spectrofluorimeter, using FLWinlab program. ThT solution (470 μL) was mixed with sample (30 μL), and the resulting fluorescence measured with parameters set as follows: excitation at 440 nm (slit 5 nm); emission at 485 nm (slit 10 nm); integration time 2 s. Biological activity was determined as percent of inhibitory activity V_i for each concentration, according to Equation (1), where F_i is the fluorescence value of the sample, F_b its blank value, and F_0 the fluorescence value of Aβ control (with the blank already subtracted).

$$V_i = 100-[(F_i-F_b)/F_0]\times 100 \quad (1)$$

© 0000 Wiley-VCH Verlag GmbH & Co. KGaA, Weinheim

Aβ aggregation kinetics: Samples for time-course experiments of Aβ(1–40) and Aβ(1–42) aggregation inhibition were prepared in PBS with 5% ethanol as co-solvent and incubated up to seven days at 37 °C. Final concentrations of Aβ and **2** were 50 μM and 25 μM, respectively. A control sample of self-aggregating Aβ was prepared in the same buffer/cosolvent conditions.

Transmission electron microscopy (TEM) studies: The samples prepared for the ThT fluorescence experiments were also used for TEM analysis. Incubated sample solution (20 μL) was applied to a carbon-coated copper/rhodium grid (400 mesh; TAAB Laboratories Equipment Ltd, Aldermaston, Berks, UK). The coated grid was floated for 2 min on the sample drop and rinsed with 200 μL of double-distilled water. Negative staining was performed with uranyl acetate solution (200 μL of 2% *w/v*; TAAB Laboratories Equipment Ltd). After draining off the excess of staining solution with filter paper, the specimen was transferred to a Philips Morgagni 282D transmission electron microscope, operating at 60 kV, for examination. Electron micrographs of negatively stained samples were photographed on Kodak electron microscope film 4489 (Kodak Company, New York, USA) and analyzed with Image 1.38 software. Statistics of fibril diameters were obtained with Kaleidagraph (Sinergy Software) calibration software.

Circular dichroism (CD) spectroscopy analysis: CD spectra were recorded in the spectral range 195–250 nm, by using 0.1 cm path length quartz cells (280 μL internal volume, from Hellma GmbH&Co KG, Milan, I) with a CD Jasco J-810 single beam spectropolarimeter. Control Aβ and Aβ/inhibitor co-incubation samples were the same as in TEM studies. CD spectra were recorded at room temperature at 0.1 nm intervals with 4 nm bandwidth and 100 nm min^{-1} scan speed. The baseline was recorded with the buffer/ethanol blank or, for co-incubation experiments, with buffer/ethanol solution of inhibitor blank, and automatically subtracted from corresponding spectra.

Bidirectional transport studies on MDCKII-MDR1 monolayers: Apical to basolateral (AP→BL) and basolateral to apical (BL→AP) permeability (P_{app}) of compounds **2** and **28** were measured using Madin–Darby canine kidney cells retrovirally transfected with human multidrug resistance gene 1 (MDCKII-MDR1). These cells were cultured in Dulbecco's modified eagle's medium (DMEM) and seeded at a density of 100 000 cell cm^{-2} onto polyester 12-well Transwell inserts (pore size 0.4 μm, 12 mm diameter, apical volume 0.5 mL, basolateral volume 1.5 mL). MDCKII-MDR1 cell barrier function was verified prior to the transport experiments by means of transepithelial electrical resistance (TEER) using an EVOM apparatus, and the measurement of the flux of fluorescein isothiocyanate-dextran (FD4, 200 μg mL^{-1}) and diazepam (75 μM) as paracellular and transcellular markers, respectively, of cell monolayers integrity and as an internal control to verify tight junction integrity during the assay. The TEER was measured in growth media (DMEM) at room temperature and calculated as the measured resistance minus the resistance of an empty Transwell (blank without cells). Cell monolayers with TEER values 800 Ohm cm^{-2} were used. Following the TEER measurements, the cells were equilibrated in transport medium in both the apical and basolateral chambers for 30 min at 37 °C. The composition of transport medium was as follows: 0.4 mM K_2HPO_4, 25 mM $NaHCO_3$, 3 mM KCl, 122 mM NaCl, 10 mM glucose, pH 7.4, and the osmolarity was 300 mOsm as determined by a freeze point based osmometer. At time 0, culture medium was aspirated from both the apical (AP) and basolateral (BL) chambers of each insert, and cell monolayers were washed three times (10 min per wash) with Dulbecco's PBS pH 7.4. Finally, a solution of compounds diluted in transport medium was added to the apical or basolateral chamber. For AP-to-BL or BL-to-AP flux studies, the drug solution was added in the AP chamber or in the BL chamber, respectively. Except for FD4, which was solubilized directly in the assay medium at a concentration of 200 μg mL^{-1}, the other compounds were first dissolved in DMSO and then diluted with the assay medium to a final concentration of 75 μM. Next, the tested solutions were added to the donor side (0.5 mL for the AP chamber and 1.5 mL for the BL chamber) and fresh assay medium was placed in the receiver compartment. The percentage of DMSO never exceeded 1% (*v/v*) in the samples. The transport experiment was carried out under cell culture conditions (37 °C, 5% CO_2, 95% humidity). After incubation time of 120 min, samples were removed from the apical and basolateral side of the monolayer and then stored until further analysis.

Quantitative analyses of compounds **2**, **28** and diazepam were performed with UV-visible spectroscopy using a PerkinElmer double-beam UV-visible spectrophotometer Lambda Bio 20 (Milan, Italy), equipped with 10 mm path-length-matched quartz cells. Standard calibration curves were prepared at maximum absorption wavelength of each compound using PBS as solvent and were linear ($r^2 = 0.999$) over the range of tested concentrations (5–100 μM). The FD4 samples were analyzed with a Victor3 fluorometer (Wallac Victor3, 1420 Multilabel Counter, PerkinElmer) at excitation and emission wavelengths of 485 and 535 nm, respectively. Each compound was tested in triplicate, and the experiments were repeated three times.

The apparent permeability (P_{app}), in cm sec^{-1}, was calculated using Equation (2), where V_A is the volume in the acceptor well, area is the surface area of the membrane, time is the total transport time, $[drug]_{acceptor}$ is the concentration of the drug measured by UV spectroscopy and $[drug]_{initial}$ is the initial drug concentration in the AP or BL chamber.

$$P_{app} = \left(\frac{V_A}{area \times time}\right) \times \left(\frac{[drug]_{acceptor}}{[drug]_{initial}}\right) \quad (2)$$

Efflux ratio (ER) was calculated using the following equation: ER = P_{app}, BL-AP/P_{app}, AP-BL, where P_{app}, BL-AP is the apparent permeability of basal-to-apical transport, and P_{app}, AP-BL is the apparent permeability of apical-to-basal transport. An efflux ratio greater than 2 indicates that a test compound is likely to be a substrate for P-gp transport.

Cytotoxicity assays: Cytotoxicity assays were carried out against human neuroblastoma cell line SH-SY5Y. Cells were maintained at 37 °C in a humidified incubator containing 5% CO_2 in DMEM (Lonza) nutrient supplemented with 10% heat inactivated fetal bovine serum, L-glutamine (2 mM), penicillin (100 U mL^{-1}) and streptomycin (100 μg mL^{-1}). Cytotoxicity of compounds was determined using the 3-(4,5-dimethylthiazol-2-yl)-2,5-diphenyl-tetrazolium bromide (MTT) assay and is expressed as IC_{50} value, the concentration that causes 50% growth inhibition. Neuroblastoma cells (10 000 cells well^{-1}) were incubated in 96-well microtiter plates overnight, then treated with a range of compound concentrations (0.1–100 μM) and incubated at 37 °C for 24 h. MTT (10 μL of 0.5% *w/v*) was added to each well, and the plates were incubated for an additional 3 h at 37 °C. Finally the cells were lysed by addition of DMSO/EtOH solution (100 μL, 1:1 *v/v*). The absorbance at 570 nm was determined using a PerkinElmer 2030 multilabel reader Victor TM X3.

© 0000 Wiley-VCH Verlag GmbH & Co. KGaA, Weinheim

Keywords: cholinesterases · amyloid-beta · multitarget agents · quinolizidines · quinonic derivatives · thioxanthenones

[1] a) R. Jakob-Roetne, H. Jacobsen, *Angew. Chem. Int. Ed.* **2009**, *48*, 3030 – 3059; *Angew. Chem.* **2009**, *121*, 3074 – 3105; b) A. Rauk, *Chem. Soc. Rev.* **2009**, *38*, 2698 – 2715; c) I. W. Hamley, *Chem. Rev.* **2012**, *112*, 5147 – 5192.

[2] a) A. Alvarez, F. Bronfman, C. A. Pérez, M. Vicente, J. Garrido, N. C. Inestrosa, *Neurosci. Lett.* **1995**, *201*, 49 – 52; b) N. C. Inestrosa, A. Alvarez, C. A. Pérez, R. D. Moreno, M. Vicente, C. Linker, O. I. Casanueva, C. Soto, J. Garrido, *Neuron* **1996**, *16*, 881 – 891; c) G. V. De Ferrari, M. A. Canales, I. Shin, L. M. Weiner, I. Silman, N. C. Inestrosa, *Biochemistry* **2001**, *40*, 10447 – 10457.

[3] a) E. Giacobini, *Drugs Aging* **2001**, *18*, 891 – 898; b) N. H. Greig, T. Utsuki, Q.-S. Yu, X. Zhu, H. W. Holloway, T. A. Perry, B. Lee, D. H. Ingram, D. K. Lahiri, *Curr. Med. Res. Opin.* **2001**, *17*, 159 – 165; c) A. L. Guillozet, J. F. Smiley, D. C. Mash, M. M. Mesulam, *Ann. Neurol.* **1997**, *42*, 909 – 918.

[4] B. Tasso, M. Catto, O. Nicolotti, F. Novelli, M. Tonelli, I. Giangreco, L. Pisani, A. Sparatore, V. Boido, A. Carotti, F. Sparatore, *Eur. J. Med. Chem.* **2011**, *46*, 2170 – 2184.

[5] a) B. J. Bayliss, A. Todrick, *Biochem. J.* **1956**, *62*, 62 – 67; b) A. Saxena, A. M. Riedman, X. Jiang, O. Lockridge, B. P. Doctor, *Biochemistry* **1997**, *36*, 14642 – 14651; c) R. Dahlbom, T. Ekstrand, *Acta Chem. Scand.* **1951**, *5*, 102 – 114; d) P. W. Elsinghorst, C. M. Gonzáles Tanarro, M. Gütschow, *J. Med. Chem.* **2006**, *49*, 7540 – 7544.

[6] a) E. V. Rozengart, *Dokl. Biochem. Biophys.* **2003**, *388*, 39 – 42 [*Chem. Abstr.* **2003**, *139*, 223727]; b) N. E. Basova, B. I. Kormilit *syn*, E. V. Rozengart, V. S. Saakov, A. A. Suvorov, *Zh. Evol. Biokhim. Fiziol.* **2012**, 48, 8 – 16 [*Chem. Abstr.* **2012**, *157*, 701122]; c) R. T. Tlegenov, Kh. Khaitbaev, É. Tilyabaev, D. N. Dalimov, A. A. Abduvakhabov, K. U. Uteniyazov, *Chem. Nat. Compd.* **1991**, *27*, 55 – 57.

[7] a) H. Mauss, *Chem. Ber.* **1948**, *81*, 19 – 31; b) S. Archer, C. M. Suter, *J. Am. Chem. Soc.* **1952**, *74*, 4296 – 4309; c) S. Archer, L. B. Rochester, M. Jackman, *J. Am. Chem. Soc.* **1954**, *76*, 588 – 591.

[8] a) S. Archer, K. J. Miller, R. Rej, C. Periana, L. Fricker, *J. Med. Chem.* **1982**, *25*, 220 – 227; b) S. Archer, R. Rej, *J. Med. Chem.* **1982**, *25*, 328 – 331; c) S. Archer, A. H. Zayed, R. Rej, T. A. Rugino, *J. Med. Chem.* **1983**, *26*, 1240 – 1246.

[9] a) M. D. Naidu, R. Agarwal, L. A. Pena, L. Cunha, M. Mezei, M. Shen, D. M. Wilson III, Y. Liu, Z. Sanchez„ P. Chaudhary, S. H. Wilson, M. J. Waring, *Plos one* **2011**, *6*, e23679; b) M. L. Fishel, M. R. Kelley, *Mol. Cell Mol. Aspects Med.* **2007**, *28*, 375 – 395.

[10] J. S. Carew, C. M. Espitia, J. A. Esquivel II, D. Mahalingam, K. R. Kelly, G. Reddy, F. J. Giles, S. T. Nawrocki, *J. Biol. Chem.* **2011**, *286*, 6602 – 6613.

[11] a) Y.-T. Tung, B.-J. Wang, M.-K. Hu, W.-M. Hsu, H. Lee, W.-P. Huang, Y.-F. Liao, *J. Biosci.* **2012**, *37*, 157 – 165; b) S. F. Funderburk, B. K. Marcellino, Z. Yue, *Mt. Sinai J. Med.* **2010**, *77*, 59 – 68.

[12] J. B. Verdier, A. D. Wolfe, *Biochem. Pharmacol.* **1986**, *35*, 1605 – 1608.

[13] R. L. Nyland, M. Luo, M. R. Kelly, R. F. Borch, *J. Med. Chem.* **2010**, *53*, 1200 – 1210.

[14] M. Necula, R. Kayed, S. Milton, C. G. Glabe, *J. Biol. Chem.* **2007**, *282*, 10311 – 10324.

[15] a) C. Glabe, *Subcell. Biochem.* **2005**, *38*, 167 – 177; b) J. Hardy, D. J. Selkoe, *Science* **2002**, *297*, 353 – 356; c) E. Gazit, *Drugs Future* **2004**, *29*, 613 – 619.

[16] R. Scherzer, E. Gazit, D. Segal, (Ramot At Tel Aviv University Ltd, Israel), PCT Int. Pat. Appl. WO 2010/026592 A1, **2010**.

[17] T. Bandiera, J. Lansen, C. Post, M. Varasi, *Curr. Med. Chem.* **1997**, *4*, 159 – 170.

[18] R. Colombo, A. Carotti, M. Catto, M. Racchi, C. Lanni, L. Verga, G. Caccialanza, E. De Lorenzi, *Electrophoresis* **2009**, *30*, 1418 – 1429.

[19] M. Pickhardt, Z. Gazova, M. von Bergen, J. Khlistunova, Y. Wang, A. Hascher, E.-M. Mandelkow, J. Biernat, E. Mandelkow, *J. Biol. Chem.* **2005**, *280*, 3628 – 3635.

[20] a) P. J. Perry, S. M. Gowan, A. P. Reszka, P. Polucci, T. C. Jenkins, L. R. Kelland, S. Neidle, *J. Med. Chem.* **1998**, *41*, 3253 – 3260; b) P. J. Perry, A. P. Reszka, A. A. Wood, M. A. Read, S. M. Gowan, N. S. Dosanjh, J. O. Trent, T. C. Jenkins, L. R. Kelland, S. Neidle, *J. Med. Chem.* **1998**, *41*, 4873 – 4884.

[21] A. Ahmed, T. Tollefsbol, *J. Am. Geriatr. Soc.* **2001**, *49*, 1105 – 1109.

[22] H. Rolyan, A. Scheffold, A. Heinrich, Y. Begus-Nahrmann, B. H. Langkopf, S. M. Hölter, D. M. Vogt-Weisenhorn, B. Liss, W. Wurst, D. C. Lie, D. R. Thal, K. Biber, K. L. Rudolph, *Brain* **2011**, *134*, 2044 – 2056.

[23] E. Nepovimova, E. Uliassi, J. Korabecny, L. E. Peña-Altamira, S. Samez, A. Pesaresi, G. E. Garcia, M. Bartolini, V. Andrisano, C. Bergamini, R. Fato, D. Lamba, M. Roberti, K. Kuca, B. Monti, M. L. Bolognesi, *J. Med. Chem.* **2014**, *57*, 8576 – 8589.

[24] S.-Y. Li, N. Jiang, S. S. Xie, K. D. Wang, X. B. Wang, L. Y. Kong, *Org. Biomol. Chem.* **2014**, *12*, 801 – 814.

[25] E. Viayna, I. Sola, M. Bartolini, A. De Simone, C. Tapia-Rojas, F. G. Serrano, R. Sabaté, J. Juárez-Jiménez, B. Pérez, F. J. Luque, V. Andrisano, M. V. Clos, N. C. Inestrosa, D. Muñoz-Torrero, *J. Med. Chem.* **2014**, *57*, 2549 – 2567.

[26] F. Leonetti, M. Catto, O. Nicolotti, L. Pisani, A. Cappa, A. Stefanachi, A. Carotti, *Bioorg. Med. Chem.* **2008**, *16*, 7450 – 7456.

[27] A. Conejo-García, L. Pisani, M. C. Núñez, M. Catto, O. Nicolotti, F. Leonetti, J. M. Campos, M. A. Gallo, A. Espinosa, A. Carotti, *J. Med. Chem.* **2011**, *54*, 2627 – 2645.

[28] H. Haviv, D. M. Wong, I. Silman, J. L. Sussman, *Curr. Top. Med. Chem.* **2007**, *7*, 375 – 387.

[29] C. Boido Canu, G. Iusco, V. Boido, F. Sparatore, A. Sparatore, *Farmaco* **1989**, *44*, 1069 – 1082.

[30] C. Boido Canu, V. Boido, F. Sparatore, *Boll. Chim. Farm.* **1989**, *128*, 208 – 211.

[31] A. Sparatore, M. Veronese, F. Sparatore, *Farmaco Ed. Sci.* **1987**, *42*, 159 – 174.

[32] E. F. Elslager, L. M. Werbel, D. F. Worth, *J. Med. Chem.* **1970**, *13*, 104 – 109.

[33] F. Ullmann, O. von Glenck, *Ber. Dtsch. Chem. Ges.* **1916**, *49*, 2487 – 2514.

[34] V. Villa, M. Tonelli, S. Thellung, A. Corsaro, B. Tasso, F. Novelli, C. Canu, A. Pino, K. Chiovitti, D. Paludi, C. Russo, A. Sparatore, A. Aceto, V. Boido, F. Sparatore, T. Florio, *Neurotoxic. Res.* **2011**, *19*, 556 – 574.

[35] F. Novelli, F. Sparatore, *Farmaco* **1993**, *48*, 1021 – 1049.

[36] V. Boido, A. Boido, C. Boido Canu, F. Sparatore, *Farmaco Ed. Sci.* **1979**, *34*, 673 – 687.

[37] H. D. H. Showalter, M. M. Angelo, E. M. Berman, G. D. Kanter, D. F. Ortwine, S. G. Ross-Kesten, A. D. Sercel, W. R. Turner, L. M. Werbel, D. F. Worth, E. F. Elslager, W. R. Leopold, J. L. Shillis, *J. Med. Chem.* **1988**, *31*, 1527 – 1539.

[38] G. L. Ellman, D. Courtney, V. Andres, R. M. Featherstone, *Biochem. Pharmacol.* **1961**, *7*, 88 – 95.

[39] S. Cellamare, A. Stefanachi, D. A. Stolfa, T. Basile, M. Catto, F. Campagna, E. Sotelo, P. Acquafredda, A. Carotti, *Bioorg. Med. Chem.* **2008**, *16*, 4810 – 4822.

[40] H. Sugimoto, H. Ogura, Y. Arai, Y. Limura, Y. Yamanishi, *Jpn. J. Pharmacol.* **2002**, *89*, 7 – 20.

[41] K. Ono, Y. Yoshiike, A. Takashima, K. Hasegawa, H. Naiki, M. Yamada, *J. Neurochem.* **2003**, *87*, 172 – 181.

[42] M. Catto, L. Pisani, F. Leonetti, O. Nicolotti, P. Pesce, A. Stefanachi, S. Cellamare, A. Carotti, *Bioorg. Med. Chem.* **2013**, *21*, 146 – 152.

[43] M. Bartolini, C. Bertucci, V. Cavrini, V. Andrisano, *Biochem Pharmacol.* **2003**, *65*, 407 – 416.

[44] M. Convertino, R. Pellarin, M. Catto, A. Carotti, A. Caflisch, *Protein Sci.* **2009**, *18*, 792 – 800.

[45] C. Brühlmann, A. Marston, K. Hostettmann, P.-A. Carrupt, B. Testa, *Chem. Biodiversity* **2004**, *1*, 819 – 829.

[46] M. T. H. Khan, I. Orhan, F. S. Şenol, M. Kartal, B. Şener, M. Dvorská, K. Šmejkal, T. Šlapetová, *Chem.-Biol. Interact.* **2009**, *181*, 383 – 389.

[47] A. Rampa, A. Bisi, P. Valenti, M. Recanatini, A. Cavalli, V. Andrisano, V. Cavrini, L. Fin, A. Buriani, P. Giusti, *J. Med. Chem.* **1998**, *41*, 3976 – 3986.

[48] L. Piazzi, F. Belluti, A. Bisi, S. Gobbi, S. Rizzo, M. Bartolini, V. Andrisano, M. Recanatini, A. Rampa, *Bioorg. Med. Chem.* **2007**, *15*, 575 – 585.

[49] S. Rizzo, A. Cavalli, L. Ceccarini, M. Bartolini, F. Belluti, A. Bisi, V. Andrisano, M. Recanatini, A. Rampa, *ChemMedChem* **2009**, *4*, 670 – 679.

[50] A. T. Petkova, Y. Ishii, J. J. Balbach, O. N. Antzutkin, R. D. Leapman, F. Delaglio, R. Tycko, *Proc. Natl. Acad. Sci. USA* **2002**, *99*, 16742 – 16747.

[51] N. Denora, V. Laquintana, A. Trapani, A. Lopedota, A. Latrofa, J. M. Gallo, G. Trapani, *Mol. Pharmaceutics* **2010**, *7*, 2255 – 2269.

[52] N. Denora, T. Cassano, V. Laquintana, A. Lopalco, A. Trapani, C. S. Cimmino, L. Laconca, A. Giuffrida, G. Trapani, *Int. J. Pharm.* **2012**, *437*, 221 – 231.

© 0000 Wiley-VCH Verlag GmbH & Co. KGaA, Weinheim

[53] F. Aruga, K. Uto, T. Fujimara, H. Kimura, T. Koike, K. Ogura, F. Sagami, *Yakuri to Chiryo* **1998**, *26*, S1163 – S1168 [*Chem. Abstr.* **1999**, *130*, 134058m].

[54] S. S. Umarova, U. B. Zakirov, I. K. Kamilov, *Farmakologiya Alkaloidov, Akad. Nauk Uzb. SSR, Inst. Khim. Rast. Veshchestv* **1965**, *2*, 258 – 263 [*Chem. Abstr.* **1967**, *66*, 53993v].

Received: March 6, 2015
Published online on ■■ ■■, 0000

© 0000 Wiley-VCH Verlag GmbH & Co. KGaA, Weinheim

"Dualing" with Alzheimer's! Thioxanthen-9-one (red), xanthen-9-one, naphtho- (green) and anthraquinone (blue) derivatives were identified as leads for the development of Alzheimer's disease therapeutics. Evaluation identified thioxanthenones **2** ($R = CH_3$, $W = (CH_2)_2$) and **4** ($R = CH_3$, $W = (CH_2)_3SCH_2$), and naphthoquinone **28** as the most potent inhibitors of Aβ aggregation, butyrylcholinesterase, and acetylcholinesterase, respectively.

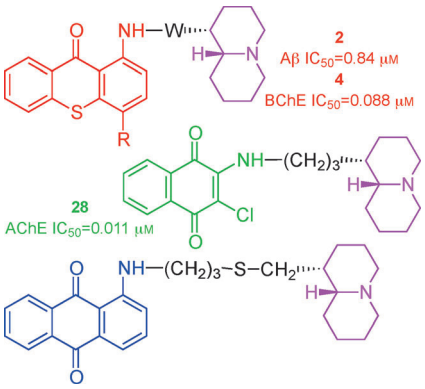

M. Tonelli, M. Catto,* B. Tasso, F. Novelli, C. Canu, G. Iusco, L. Pisani, A. D. Stradis, N. Denora, A. Sparatore, V. Boido, A. Carotti, F. Sparatore*

■■ – ■■

Multitarget Therapeutic Leads for Alzheimer's Disease: Quinolizidinyl Derivatives of Bi- and Tricyclic Systems as Dual Inhibitors of Cholinesterases and β-Amyloid (Aβ) Aggregation

© 0000 Wiley-VCH Verlag GmbH & Co. KGaA, Weinheim